Available online at www.sciencedirect.com
ScienceDirect
Journal of Organometallic Chemistry 691 (2006) 4514–4531
Journal of Organometallic Chemistry
www.elsevier.com/locate/jorganchem

Electronic communication between tungsten alkylidyne and metal isocyanide complex fragments across phenyleneethynylene bridges

Marie Pui Yin Yu [a], Vivian Wing-Wah Yam [a,*], Kung-Kai Cheung [a], Andreas Mayr [b,*]

[a] *Department of Chemistry, The University of Hong Kong, Pokfulam Road, Hong Kong, China*
[b] *Department of Chemistry, State University of New York at Stony Brook, Stony Brook, NY 11794-3400, USA*

Received 28 December 2005; received in revised form 17 February 2006; accepted 20 February 2006
Available online 28 February 2006

Abstract

Heteronuclear metal complexes of the type $[X(CO)_2(LL)W{\equiv}C(-C_6H_4-C{\equiv}C)_p-C_6H_4-N{\equiv}C-]_nML_m$ (X = Cl, Br; LL = tmeda, dppe; $p = 0$–3; $n = 1$ for $Cr(CO)_5$, $n = 2$ for $ReX(CO)_3$, $PdCl_2$, PdI_2, and PtI_2) have been prepared. The molecular structure of one example, $[Cl(CO)_2(tmeda)W{\equiv}C-C_6H_4-N{\equiv}C-]_2PdI_2$, was determined by X-ray crystallography. The extent of electronic communication between the tungsten alkylidyne and the metal isocyanide centers was probed by various spectroscopic techniques. In the parent systems ($p = 0$), the electronic changes due to modification of the isocyanide metal complex fragments could be distinguished clearly by the ^{13}C NMR chemical shift of the alkylidyne carbon atom and the $d \rightarrow \pi^*$ and $\pi \rightarrow \pi^*$ electronic transitions of the metal alkylidyne system. However, only residual effects could be discerned for the longer systems using these spectroscopic probes. Probes based on the emission property of the tungsten alkylidyne fragment proved to be the most useful in distinguishing long-range effects in those cases where the isocyanide metal complex fragment is capable of quenching the emission. This is the case for $ML_m = PdCl_2$ and PdI_2. Partial quenching effects were still observed at the longest investigated distance between the metal centers of about 3.1 nm. The available evidence suggests that the quenching mechanism is electron transfer.

Keywords: Tungsten alkylidyne complex; Metal isocyanide complex; Photoluminescence; Electron transfer

1. Introduction

Methods to establish electronic communication between molecular entities across extended distances are of central importance to the development of molecular devices for applications such as energy conversion, sensing, or molecular electronics [1]. The mechanism of interaction may be electron transfer, energy transfer, or the change of some spectroscopic or structural parameter upon modification of one of the interacting sites [2]. The particular mechanism is primarily determined by the nature of the interacting sites, but the molecular bridge between them also plays a crucial role, especially in determining the efficiency of communication [3].

Transition metal centers are among the most versatile active components for establishing electronic communication [4] and unsaturated organic systems have proven to be among the most useful bridging units [5]. In this study, we explore the electronic interactions between tungsten alkylidyne and metal isocyanide complex fragments across phenyleneethynylene bridges [6]. Metal alkylidynes are characterized by the presence of strong metal–carbon triple bonds [7], and several dinuclear complexes with bridging conjugated bis(alkylidyne) ligands have been prepared [8]. In addition, alkylidyne metal complexes possess photophysical properties which may make them useful as active molecular device components [9]. The

* Corresponding authors. Tel.: +852 2859 2153; fax: +852 2857 1586 (V.W.-W. Yam); tel.: +1 631 632 7951; fax: +1 631 632 7960 (A. Mayr).
E-mail addresses: wwyam@hku.hk (V.W.-W. Yam), amayr@notes.cc.sunysb.edu (A. Mayr).

0022-328X/$ - see front matter © 2006 Elsevier B.V. All rights reserved.
doi:10.1016/j.jorganchem.2006.02.029

metal–isocyanide linkage is also characterized by the presence of metal–carbon π interactions, albeit much weaker ones than those in metal alkylidynes [10]. The advantage of the metal isocyanide system, in the context of this study, is the possibility to attach metal complex fragments with a wide range of electronic properties [11,12]. These two different types of metal complex fragment are connected via phenyleneethynylene units. Oligo(phenyleneethynylene)s (OPE) are widely used as bridges, not only because of their good electronic transmission properties [13], but also for their strictly linear geometry and ease of preparation [14]. With the attachment of M≡C– and –N≡C–M′ groups to the ends of OPE chains the metal centers not only terminate, but become integral parts of extended π systems. In such α,ω-dimetalla-π-systems the exchange of electronic information between the metal centers may be expected to be particularly efficient. The present heteronuclear metal complexes are members of a growing family of carbon- and hydrocarbon-bridged metal complexes in which the metal centers are connected directly, via metal–carbon σ/π bonds, to the ends of extended π systems [15].

2. Experimental

Standard inert atmosphere techniques were used throughout. Diethyl ether, hexane and THF were purified by reflux over sodium and distillation. Methylene chloride was heated to reflux over calcium hydride and distilled. 4-Iodophenyltrimethylsilylacetylene, 2,6-diisopropylphenylisocyanide, and compounds **1**, **5**, and **7**–**9** as well as **10** and **11** were prepared as previously reported [16,17]. ^{1}H, $^{13}C\{^{1}H\}$ and $^{31}P\{^{1}H\}$ NMR spectra were recorded on 270 MHz JEOL JNMGSX270 FT-NMR, 300 MHz BRUKER DPX300 FT-NMR and 500 MHz BRUKER DRX500 FT-NMR spectrometers. ^{1}H and $^{13}C\{^{1}H\}$ NMR chemical shifts are given in ppm (δ) relative to $SiMe_4$. $^{31}P\{^{1}H\}$ NMR spectra are referenced to 85% H_3PO_4. IR spectra were recorded on a Shimadzu FT-IR-8201PC spectrometer. UV/Vis absorption spectra were recorded on a Hewlett–Packard 8452A diode array spectrophotometer. Emission spectra were recorded on a Spex Fluorolog 111 spectrofluorometer. Solutions were degassed with not less than four freeze–pump–thaw cycles. Emission lifetime measurements were performed using a conventional laser system. The excitation source was the 355-nm output (third harmonic) of a Quanta-Ray Q-switched GCR-150 pulsed Nd-YAG laser (10 Hz). Luminescence decay signals were recorded on a Tektronix model TDS-620A (500 MHz, 2GS/s) digital oscilloscope, and analyzed using a program for exponential fits. The relative luminescence quantum yields were measured at room temperature by the Parker–Rees method [18]. $[Ru(bpy)_3]Cl_2$ in deionized water has been used as the reference and all samples were irradiated at 453 nm since all complexes absorb strongly in this region. The refractive index of the sample and the reference solutions were 1.344 and 1.333, respectively. The luminescence quantum yield of the reference was 0.055 with irradiation at 453 nm [19]. Cyclic voltammetric measurements were performed by using a CH Instrument Inc., model CHI 620 Electroanalytical Analyzer, interfaced to a personal computer. The ferrocenium–ferrocene couple was used as the internal standard in the electrochemical measurements in acetonitrile (0.1 M $^{n}Bu_4NPF_6$) (0.38 V versus SCE) [20]. The working electrode was a glassy carbon (Atomergic Chemetals V25) electrode, $Ag/AgNO_3$ (0.1 M in CH_3CN) as the reference electrode and with a platinum foil acting as the counter electrode. Melting points were recorded on a Stuart Scientific SMP1 instrument under nitrogen. Elemental analyses were performed by Butterworth Laboratories Ltd.

2.1. Synthesis of compound 2

Compound **1** (2.04 g, 6.10 mmol) and 2.23 g of 4-$IC_6H_4CCSiMe_3$ (2.23 g, 7.43 mmol) were dissolved in NEt_3 (100 mL), and $PdCl_2(PPh_3)_2$ (40 mg 0.057 mmol) and CuI (40 mg, 0.21 mmol) were added. The resulting solution was stirred at 40 °C overnight. The solvent was then removed and the residue was dissolved in CH_2Cl_2. This organic solution was washed with water. The organic extract was dried, and the solvent was removed under reduced pressure. The product was purified by column chromatography on silica gel using hexane as the eluent. Removal of the solvent yielded a pale yellow crystalline solid. Yield: 2.49 g, 80%. The terms minor isomer and major isomer in the lists of NMR data refer to the conformational isomers of the formamide group. ^{1}H NMR ($CDCl_3$): δ 8.48 (s, 1H, minor isomer, NHC*H*O), 8.04 (d, $J = 11.8$ Hz, 1H, major isomer, NHC*H*O), 7.53–7.37 (10H, C_6H_4CC, C_6H_2i-Pr_2), 7.12 (d, $J = 11.8$ Hz, 1H, major isomer, N*H*CHO), 6.79 (s, 1H, minor isomer, N*H*CHO), 3.25–3.16 (m, 2H, major isomer, C*H*CH_3), 3.14–3.06 (m, 2H, minor isomer, C*H*CH_3), 1.24 (d, $J = 6.8$ Hz, 12H, CHC*H*$_3$), 0.26 (s, 9H, SiC*H*$_3$). $^{13}C\{^{1}H\}$ NMR ($CDCl_3$): δ 164.8 (NH*C*HO, major isomer), 160.4 (NH*C*HO, minor isomer), 146.9, 146.5, 131.9, 131.6, 131.5, 131.4, 130.2, 129.9, 127.3, 127.1, 123.5, 123.4, 123.2, 123.1, 123.0, 122.8 (C_6H_4CC, C_6H_2i-Pr_2), 104.6, 96.5, 91.0, 90.9, 89.4, 89.0 (*C*≡*C*), 28.8, 28.4 (*C*HCH$_3$), 23.5 (CH*C*H$_3$), 0 (Si*C*H$_3$). IR (CH_2Cl_2, cm^{-1}): 2156 (w, $\nu_{C\equiv CSi}$). mp 182–185 °C. MS (EI): 501 (M^+).

2.2. Synthesis of compound 3

Compound **2** (0.501 g, 1 mmol) was dissolved in MeOH (100 mL) and KOH (0.5 g) was added. The solution was stirred at r.t. for 2 h. The solvent was then removed, and the residue was dissolved in CH_2Cl_2. The organic solution was washed with water. The organic extract was dried, and the solvent was removed to give a pale yellow crystalline solid. Yield: 0.408 g, 95%. ^{1}H

NMR ($CDCl_3$): δ 8.48 (s, 1H, minor isomer, NHC*H*O), 8.04 (d, $J = 11.8$ Hz, 1H, major isomer, NHC*H*O), 7.56–7.37 (10H, C_6H_4CC, C_6H_2i-Pr_2), 7.18 (d, $J = 11.8$ Hz, 1H, major isomer, N*H*CHO), 6.82 (s, 1H, minor isomer, N*H*CHO), 3.25–3.20 (m, 2H, major isomer, CHCH_3), 3.19 (s, 1H, C≡C*H*), 3.16–3.06 (m, 2H, minor isomer, C*H*CH3), 1.24 (d, $J = 6.8$ Hz, 12H, CHCH_3). $^{13}C\{^1H\}$ NMR ($CDCl_3$): δ 164.8 (NH*C*HO, major isomer), 160.4 (NH*C*HO, minor isomer), 146.9, 146.5, 132.1, 131.6, 131.5, 130.2, 129.9, 127.3, 127.1, 123.5, 123.4, 123.3, 123.1, 127.1, 123.5, 123.4, 123.3, 123.1, 123.0, 122.7, 122.1 (C_6H_4CC, C_6H_2i-Pr_2), 91.5, 91.0, 90.8, 89.4, 89.0 (*C*≡*C*), 83.2 (C≡*C*H), 28.8, 28.5 (*C*HCH$_3$), 23.5 (CH*C*H$_3$). IR (CH_2Cl_2, cm^{-1}): 2108 (w, $\nu_{C\equiv CH}$). mp 197–200 °C. MS (EI): 429 (M^+).

2.3. Synthesis of compound 4

Compound **3** (0.429 g, 1.00 mmol) was dissolved in CH_2Cl_2 (30 mL), and NEt_3 (2 mL) was added. A CH_2Cl_2 solution of triphosgene (0.15 g, 50% excess) was added at −78 °C. The mixture was warmed to r.t. and stirred for 2 h. Water was then added to the solution to destroy the excess triphosgene. The organic layer was dried, and the solvent was removed to give a yellow crystalline solid. Yield: 0.354 g, 86%. ^1H NMR ($CDCl_3$): δ 7.53 (s, 4H, C_6H_4CC), 7.48 (s, 4H, C_6H_4CC), 3.42–3.33 (m, 2H, CHCH$_3$), 3.19 (s, 1H, CC*H*), 1.30 (d, $J = 6.9$ Hz, 12H, CH$_3$). $^{13}C\{^1H\}$ NMR ($CDCl_3$): δ 170.1 (N≡*C*), 145.3, 132.1, 131.6, 131.5, 126.7, 124.1, 123.4, 123.2, 122.8, 122.2 (C_6H_4CC, C_6H_2i-Pr_2), 90.9, 90.8, 90.6 (*C*≡*C*), 83.2 (*C*CH), 79.1 (C*C*H). IR (CH_2Cl_2, cm^{-1}): 2118 (s, $\nu_{C\equiv N}$). mp 140–143 °C.

2.4. Synthesis of compound 6

Compound **5** (1.78 g, 2.00 mmol) was dissolved in THF (30 mL), and $HNEt_2$ (4 mL) was added. To this solution, compound **3** (1.03 g, 1.47 mmol), *cis*-$PdCl_2(PPh_3)_2$ (20 mg), and CuI (20 mg) were added to this solution. The resulting mixture was stirred at r.t. overnight. The solvent was removed in vacuo. The residue was washed with hexane, dried, and redissolved in CH_2Cl_2. After filtration, hexane was added to the solution to afford yellow-orange micro-crystals. Yield: 1.56 g, 65%. ^1H NMR ($CDCl_3$): δ 8.47 (s, 1H, NHC*H*O, minor isomer), 8.04 (d, $J = 11.8$ Hz, 1H, NHC*H*O, major isomer), 7.75–7.19 (30H, P*Ph*$_2$, C_6H_4, C_6H_2i-Pr_2), 7.10 (d, $J = 8.3$ Hz, 2H, CC_6H_4), 6.91 (d, $J = 11.8$ Hz, 1H, N*H*CHO, major isomer), 6.74 (s, 1H, N*H*CHO, minor isomer), 6.45 (d, $J = 8.3$ Hz, 2H, CC_6H_4), 3.25–3.13 (m, 2H, C*H*(CH$_3$)$_2$), 3.10–2.84 (m, 2H, CH_2PPh$_2$), 2.73–2.58 (m, 2H, CH_2PPh$_2$), 1.24 (d, $J = 6.8$ Hz, 12H, CH$_3$). $^{13}C\{^1H\}$ NMR ($CDCl_3$): δ 164.7 (NH*C*HO, major isomer), 160.4 (NH*C*HO, minor isomer), 146.9, 146.5, 135.9, 135.3, 133.0, 132.8, 132.7, 132.5, 132.1, 131.6, 131.4, 130.6, 130.3, 130.1, 129.4, 128.6, 128.5, 127.3, 127.1, 123.3, 123.2, 123.0, 122.9, 121.3 (P*Ph*$_2$, CC_6H_4CC, C_6H_4, C_6H_2i-Pr_2), 91.3, 91.1, 91.0, 89.5 (*C*≡*C*), 28.8, 28.5 (*C*H(CH$_3$)$_2$), 27.6, 27.2, 27.0 (*C*H$_2$PPh$_2$), 23.5 (*C*H$_3$). $^{31}P\{^1H\}$ NMR ($CDCl_3$): δ 39.2 ($^1J_{WP} = 231$ Hz). IR (CH_2Cl_2, cm^{-1}): 2008 (s, ν_{CO}), 1940 (s, ν_{CO}), 1697 (m, $\nu_{C=O}$). UV (CH_2Cl_2, nm) (ε, $M^{-1}\,cm^{-1}$): 460 (1500, sh), 380 (77 000). mp 150–153 °C (dec.).

2.5. Synthesis of compound 12

Compound **6** (0.300 g, 0.252 mmol) was dissolved in CH_2Cl_2 (50 mL), and 0.56 mL NEt_3 was added. After cooling to −78 °C, a solution of triphosgene (50 mg) in CH_2Cl_2 (10 mL) was added. The resulting mixture was allowed to warm to 0 °C and stirred for 30 min. The solvent was then removed in vacuo. The residue was washed with hexane and redissolved in THF (30 mL). After filtration, the solvent was removed in vacuo. The residue was redissolved in CH_2Cl_2. After filtration, hexane was added to the solution to afford yellow-orange crystals. Yield: 0.136 g, 46%. ^1H NMR ($CDCl_3$): δ 7.75–7.65 (8H, P*Ph*$_2$), 7.56–7.20 (26H, P*Ph*$_2$, C_6H_4CC, C_6H_2i-Pr_2), 7.10 (d, $J = 8.3$ Hz, 2H, CC_6H_4), 6.45 (d, $J = 8.3$ Hz, 2H, CC_6H_4), 3.37 (hept, $J = 6.9$ Hz, 2H, C*H*CH$_3$), 3.01–2.84 (m, 2H, CH_2PPh$_2$), 2.75–2.56 (m, 2H, CH_2PPh$_2$), 1.30 (d, $J = 6.9$ Hz, 12H, CH$_3$). $^{13}C\{^1H\}$ NMR ($CDCl_3$): δ 265.0 (W≡*C*), 212.3 (*C*O, $^1J_{PC}^{cis} = 7.0$ Hz, $^1J_{PC}^{trans} = 46.0$ Hz), 170.4 (N≡*C*), 149.0, 145.3, 135.5, 133.0, 132.9, 132.7, 132.6, 132.5, 132.4, 131.7, 131.6, 131.5, 130.6, 130.3, 130.1, 129.5, 128.6, 128.5, 128.4, 128.3, 126.8, 126.7, 124.2, 123.4, 123.3, 122.9, 121.4 (CC_6H_4, C_6H_4CC, C_6H_2i-Pr_2), 92.0, 91.3, 91.0, 90.8, 90.7 (*C*≡*C*), 29.9, 27.5, 27.4, 27.3, 27.2 (*C*H$_2$PPh$_2$), 22.5 (*C*H$_3$). $^{31}P\{^1H\}$ NMR ($CDCl_3$): δ 39.2 ($^1J_{WP} = 231$ Hz). IR (CH_2Cl_2, cm^{-1}): 2116 (m, ν_{CN}), 2008 (s, ν_{CO}), 1940 (s, ν_{CO}). mp 165–168 °C (dec.).

2.6. Synthesis of compound 13

A suspension of $Cr(CO)_6$ (0.050 g, 0.227 mmol) in THF (20 mL) was irradiated by a UV lamp for 2 h and then transferred to a solution of **7** (0.115 g, 0.227 mmol) in THF (30 mL) at 0 °C. The resulting mixture was stirred at 0 °C for 3 h, and the solvent was removed in vacuo. The residue was washed with hexane, dried, and redissolved in CH_2Cl_2. After filtration, hexane was added to the solution to afford a light orange precipitate. Yield: 0.05 g, 33%. ^1H NMR ($CDCl_3$): δ 7.23–7.21 (4H, C_6H_4NC), 3.21 (s, 6H, NCH_3), 3.06–2.92 (br, 4H, NCH_2), 2.96 (s, 6H, NCH_3). $^{13}C\{^1H\}$ NMR ($CDCl_3$): δ 257.3 (W≡*C*), 220.4 (*C*O), 216.4, 214.3 (Cr-*C*O), 149.3, 130.2, 126.2, 125.9 (C_6H_4NC), 61.1, 58.2, 52.3 (*C*H$_2$N(*C*H$_3$)$_2$). IR (CH_2Cl_2, cm^{-1}): 2137 (m, ν_{CN}), 2056 (s, ν_{Cr-CO}), 1990 (s, ν_{CO}), 1956 (vs, ν_{Cr-CO}), 1902 (s, ν_{CO}). Anal. Calc. for $C_{21}H_{20}ClCrN_3O_7W$: C, 36.15; H, 2.89; N, 6.02. Found: C, 36.14; H, 2.92; N, 5.98%. mp 165–170 °C (dec.).

2.7. Synthesis of compound **14**

A solution of $ReCl(CO)_5$ (50 mg, 0.14 mmol) in THF (100 mL) was stirred under reflux overnight. Then **7** (0.15 g, 0.30 mmol) was added. The resulting mixture was stirred at r.t. for 1 h, and the solvent was removed in vacuo. The residue was washed with hexane, dried, and redissolved in CH_2Cl_2. After filtration, hexane was added to the solution to afford a light orange precipitate. Yield: 0.118 g, 73%. ^1H NMR (CD_2Cl_2): δ 7.36 (d, $J = 8.6$ Hz, 2H, C_6H_4NC), 7.27 (d, $J = 8.6$ Hz, 2H, C_6H_4NC), 3.18 (s, 6H, NCH_3), 2.95–2.88 (br, 4H, NCH_2), 2.91 (s, 6H, NCH_3). $^{13}C\{^1H\}$ NMR (CD_2Cl_2): δ 257.5 (W≡*C*), 221.5 (*C*O), 187.6, 184.6 (Re*C*O), 150.8, 130.6, 127.1, 124.5 (C_6H_4NC), 61.4, 58.5 ($CH_2N(CH_3)_2$). IR (CH_2Cl_2, cm^{-1}): 2185 (w, ν_{CN}), 2151 (m, ν_{CN}), 2039 (s, ν_{Re-CO}), 1992 (s, ν_{CO}), 1933 (m, ν_{Re-CO}), 1904 (s, ν_{CO}). Anal. Calc. for $C_{35}H_{40}Cl_3N_6O_7ReW_2$: C, 31.92; H, 3.06; N, 6.38. Found: C, 31.88; H, 2.79; N, 6.08%. mp 190–195 °C (dec.).

2.8. Synthesis of compound **15**

The synthesis follows the procedure described for **14**, whereby $ReBr(CO)_5$ and **8** were used. Light-orange precipitate. Yield: 56%. ^1H NMR (CD_2Cl_2): δ 7.37 (d, $J = 8.6$ Hz, 2H, C_6H_4NC), 7.32 (d, $J = 8.6$ Hz, 2H, C_6H_4NC), 3.24 (s, 6H, NCH_3), 3.04 (s, 6H, NCH_3), 2.95 (m, 4H, $CH_2N(CH_3)_2$). $^{13}C\{^1H\}$ NMR (CD_2Cl_2): δ 258.1 (W≡*C*), 221.4 (*C*O), 187.1, 184.7 (Re*C*O), 150.7, 131.2, 127.7, 125.3 (C_6H_4NC), 62.1, 59.2 ($CH_2N(CH_3)_2$). IR (CH_2Cl_2, cm^{-1}): 2181 (w, ν_{CN}), 2151 (m, ν_{CN}), 2037 (s, ν_{Re-CO}), 1992 (s, ν_{CO}), 1935 (m, ν_{Re-CO}), 1904 (s, ν_{CO}). Anal. Calc. for $C_{35}H_{40}BrCl_2N_6O_7ReW_2 \cdot 0.25C_6H_{14}$: C, 29.44; H, 2.81; N, 5.64. Found: C, 29.43; H, 2.47; N, 5.74%. mp 190–195 °C (dec.).

2.9. Synthesis of compound **16**

To a suspension of $PdCl_2$ (25 mg) in THF (30 mL), compound **7** (0.118 g) was added. The mixture was stirred at r.t. overnight, and the solvent was removed in vacuo. The residue was washed with hexane, dried, and redissolved in CH_2Cl_2. After filtration, hexane was added to the solution to afford a yellow-orange crystalline solid. Yield: 32%. ^1H NMR (CD_2Cl_2): δ 7.42 (d, $J = 8.5$ Hz, 2H, CC_6H_4), 7.29 (d, $J = 8.5$ Hz, 2H, CC_6H_4), 3.18 (s, 6H, NCH_3), 2.91 (s, 6H, NCH_3), 3.00–2.86 (br, 4H, NCH_2). $^{13}C\{^1H\}$ NMR (CD_2Cl_2): δ 256.3 (W≡*C*), 221.4 (*C*O), 152.1, 130.7, 127.2, 122.9 (CC_6H_4), 61.5, 58.6 (CH_3NCH_2). IR (CH_2Cl_2, cm^{-1}): 2228 (w, ν_{CN}), 2212 (w, ν_{CN}), 1994 (s, ν_{CO}), 1906 (s, ν_{CO}). mp 147–150 °C (dec.).

2.10. Synthesis of compound **17**

A solution of **7** (0.5 mmol) in THF (50 mL) was transferred to a supsension of PdI_2(0.22 mmol, 0.079 g) in THF (20 mL). The mixture was stirred at 0 °C for 1 h. After filtration, the solvent was removed in vacuo. The residue was washed with hexane, dried, and redissolved in CH_2Cl_2. After filtration, hexane was added to the solution to afford **7** as dull red crystals. Yield: 66%. ^1H NMR ($CDCl_3$): δ 7.39 (d, $J = 8.6$ Hz, 2H, C_6H_4NC), 7.26 (d, $J = 8.6$ Hz, 2H, C_6H_4NC), 3.21 (s, 6H, NCH_3), 3.03–2.86 (br, 4H, NCH_2), 2.96 (s, 6H, NCH_3). $^{13}C\{^1H\}$ NMR ($CDCl_3$): δ 256.0 (W≡*C*), 220.2 (*C*O), 151.3, 130.2, 126.5, 122.9 (C_6H_4NC), 61.1, 58.3, 52.4 ($CH_2N(CH_3)_2$). IR (CH_2Cl_2, cm^{-1}): 2199 (m, ν_{CN}), 1992 (s, ν_{CO}), 1906 (s, ν_{CO}). Anal. Calc. for $C_{32}H_{40}Cl_2I_2N_6O_4PdW_2$: C, 28.02; H, 2.94; N, 6.13. Found: C, 27.97; H, 2.98; N, 5.95%. mp 163–170 °C (dec.).

2.11. Synthesis of compound **18**

The synthesis follows the procedure described for **17**, whereby PtI_2 was used instead of PdI_2. The mixture of **7** and PtI_2 was stirred at 0 °C overnight. A subsequent workup procedures similar to that of **17** afforded **18** as red crystals. Yield: 46%. ^1H NMR ($CDCl_3$): δ 7.38 (d, $J = 8.5$ Hz, 2H, C_6H_4NC), 7.26 (d, $J = 8.5$ Hz, 2H, C_6H_4NC), 3.21 (s, 6H, NCH_3), 3.01–2.88 (m, 4H, NCH_2), 2.96 (s, 6H, NCH_3). $^{13}C\{^1H\}$ NMR ($CDCl_3$): δ 256.1 (W≡*C*), 220.2 (*C*O), 151.2, 130.2, 126.6, 123.1 (C_6H_4NC), 61.1, 58.3, 52.4 ($CH_2N(CH_3)_2$). IR (CH_2Cl_2, cm^{-1}): 2193 (m, ν_{CN}), 1994 (s, ν_{CO}), 1904 (s, ν_{CO}). Anal. Calc. for $C_{32}H_{40}Cl_2I_2N_6O_4PtW_2$: C, 26.32; H, 2.76; N, 5.76. Found: C, 26.18; H, 2.84; N, 5.69%. mp 170–180 °C (dec.).

2.12. Synthesis of compound **19**

The synthesis follows the procedure described for **14**, whereby **9** was used. Light-orange precipitate. Yield: 64%. ^1H NMR ($CDCl_3$): δ 7.74–7.20 (20H, PPh_2), 7.01 (d, $J = 8.5$ Hz, 2H, C_6H_4NC), 6.41 (d, $J = 8.5$ Hz, 2H, C_6H_4NC), 3.01–2.89 (m, 2H, CH_2PPh_2), 2.74–2.62 (m, 2H, CH_2PPh_2). $^{13}C\{^1H\}$ NMR ($CDCl_3$): δ 260.6 (W≡*C*), 211.9 (*C*O, $^1J_{PC}^{cis} = 6.0$ Hz, $^1J_{PC}^{trans} = 46.0$ Hz), 186.5, 184.0 (Re*C*O), 150.4, 146.0, 136.0, 135.4, 133.0, 132.9, 132.7, 132.6, 132.5, 132.3, 132.2, 132.0, 131.7, 130.5, 130.3, 130.0, 128.7, 128.6, 128.3, 126.2, 126.1, 123.6 (PPh_2, C_6H_4NC), 27.5, 27.3, 27.1, 26.9 (CH_2PPh_2). ^{31}P NMR ($CDCl_3$): δ 38.0 ($^1J_{WP} = 232$ Hz). IR (CH_2Cl_2, cm^{-1}): 2185 (w, ν_{CN}), 2149 (m, ν_{CN}), 2039 (s, ν_{Re-CO}), 2012 (s, ν_{CO}), 1994 (s, ν_{Re-CO}), 1944 (s, ν_{CO}). mp 168–170 °C (dec.).

2.13. Synthesis of compound **20**

Compound **9** (0.14 g) was added to a suspension of PdI_2(48 mg) in THF (50 mL). The resulting mixture was stirred at r.t. for 24 h. After filtration, the solvent was removed in vacuo. The residue was washed with hexane, dried, and redissolved in CH_2Cl_2. After filtration, hexane was added to the solution to afford orange micro-crystals.

Yield: 25%. ^{1}H NMR ($CDCl_3$): δ 7.74–7.22 (20H, P*Ph*$_2$), 7.05 (d, $J = 8.6$ Hz, 2H, C_6H_4NC), 6.40 (d, $J = 8.6$ Hz, 2H, C_6H_4NC), 3.02–2.87 (m, 2H, CH_2PPh$_2$), 2.78–2.64 (m, 2H, CH_2PPh$_2$). ^{13}C{^{1}H} NMR ($CDCl_3$): δ 260.0 (W≡*C*), 211.8 (*C*O, $^1J_{PC}^{cis} = 7.0$ Hz, $^1J_{PC}^{trans} = 46.0$ Hz), 151.4, 135.9, 135.6, 133.0, 132.9, 132.8, 132.6, 132.8, 132.4, 132.3, 132.0, 130.5, 130.4, 130.3, 130.2, 128.9, 128.8, 128.7, 128.6, 128.5, 128.4, 128.0, 125.9, 125.7, 122.6 (P*Ph*$_2$, C_6H$_4$NC), 27.5, 27.4, 27.2, 27.1 (*C*H$_2$PPh$_2$). ^{31}P NMR ($CDCl_3$): δ 37.8 ($^1J_{WP} = 232$ Hz). IR (CH_2Cl_2, cm^{-1}): 2199 (m, ν_{CN}), 2014 (s, ν_{CO}), 1946 (s, ν_{CO}). mp 150–152 °C (dec.).

2.14. Synthesis of compound **21**

The synthesis follows the procedure described for **20**, whereby PtI_2 was used. The mixture of **9** and PtI_2 was stirred at r.t. for 2 h to afford **21** as orange microcrystals. Yield: 0.13 g, 72%. ^{1}H NMR ($CDCl_3$): δ 7.74–7.21 (20H, P*Ph*$_2$), 7.04 (d, $J = 8.6$ Hz, 2H, C_6H_4NC), 6.40 (d, $J = 8.6$ Hz, 2H, C_6H_4NC), 3.02–2.86 (m, 2H, CH_2PPh$_2$), 2.80–2.62 (m, 2H, CH_2PPh$_2$). ^{13}C{^{1}H} NMR ($CDCl_3$): δ 260.1 (W≡*C*), 211.8 (*C*O, $^1J_{PC}^{cis} = 7.0$ Hz, $^1J_{PC}^{trans} = 46.0$ Hz), 184.3 (N≡*C*), 151.3, 135.9, 135.6, 134.1, 134.0, 133.0, 132.9, 132.8, 132.6, 132.5, 132.4, 132.3, 132.0, 130.5, 130.4, 130.3, 130.2, 128.8, 128.7, 128.6, 128.5, 128.4, 126.0, 125.9, 122.8 (P*Ph*$_2$, C_6H$_4$NC), 27.5, 27.4, 27.3, 27.2 (*C*H$_2$PPh$_2$). ^{31}P NMR ($CDCl_3$): δ 37.8 ($^1J_{WP} = 232$ Hz). IR (CH_2Cl_2, cm^{-1}): 2191 (m, ν_{CN}), 2014 (s, ν_{CO}), 1946 (s, ν_{CO}). mp 170–172 °C (dec.).

2.15. Synthesis of compound **22**

$ReCl(CO)_5$ (20 mg) was dissolved in THF (30 mL) and stirred under reflux overnight. Then 0.118 g (20% excess) of **10** was added. The resulting mixture was stirred at r.t. for 4 h. The solvent was removed in vacuo. The residue was washed with hexane, dried, and redissolved in CH_2Cl_2. After filtration, hexane was added to the solution to afford orange micro-crystals. Yield: 50 mg (43%). ^{1}H NMR ($CDCl_3$): δ 7.72–7.59 (8H, *PPh*$_2$), 7.56 (d, $J = 8.7$ Hz, 2H, C_6H_4NC), 7.47 (d, $J = 8.7$ Hz, 2H, C_6H_4NC), 7.44–7.15 (12H, P*Ph*$_2$), 7.10 (d, $J = 8.3$ Hz, 2H, C_6H_4CC), 6.46 (d, $J = 8.3$ Hz, 2H, C_6H_4CC), 2.95–2.88 (m, 2H, CH_2PPh$_2$), 2.71–2.59 (m, 2H, CH_2PPh$_2$). ^{13}C{^{1}H} NMR ($CDCl_3$): δ 264.5 (W≡*C*), 211.9 (*C*O, $^1J_{PC}^{cis} = 8.0$ Hz), 186.3, 183.9 (Re*C*O), 149.3, 146.6, 135.9, 135.3, 134.1, 133.5, 133.0, 132.9, 132.8, 132.7, 132.5, 132.4, 132.3, 132.0, 131.0, 130.8, 130.7, 130.6, 130.5, 130.3, 130.1, 129.5, 129.2, 128.9, 128.8, 128.6, 128.5, 128.4, 128.3, 127.1, 127.0, 125.6, 120.4 (P*Ph*$_2$, C_6H$_4$NC, C_6H$_4$CC), 93.6, 89.7 (*C*≡*C*), 27.6, 27.4, 27.2, 27.0 (*C*H$_2$PPh$_2$). ^{31}P NMR ($CDCl_3$): δ 39.2 ($^1J_{WP} = 231$ Hz). IR (CH_2Cl_2, cm^{-1}): 2210 (w, $\nu_{C\equiv C}$), 2185 (w, ν_{CN}), 2151 (m, ν_{CN}), 2039 (s, ν_{Re-CO}), 2008 (s, ν_{CO}), 1994 (s, ν_{Re-CO}), 1940 (s, ν_{CO}). mp 150–153 °C (dec.).

2.16. Synthesis of compound **23**

The synthesis follows the procedure described for **20**, using **10** and PdI_2. Orange-yellow micro-crystals. Yield: 30%. ^{1}H NMR ($CDCl_3$): δ 7.75–7.61 (8H, P*Ph*$_2$), 7.59 (d, $J = 6.8$ Hz, 2H, C_6H_4NC), 7.52 (d, $J = 6.8$ Hz, C_6H_4NC), 7.50–7.20 (12H, P*Ph*$_2$), 7.11 (d, $J = 8.3$ Hz, 2H, C_6H_4CC), 6.46 (d, $J = 8.3$ Hz, 2H, C_6H_4CC), 2.97–2.89 (m, 2H, CH_2PPh$_2$), 2.72–2.64 (m, 2H, CH_2PPh$_2$). ^{13}C{^{1}H} NMR ($CDCl_3$): δ 264.5 (W≡*C*), 212.2 (*C*O, $^1J_{PC}^{cis} = 6.0$ Hz, $^1J_{PC}^{trans} = 46.0$ Hz), 149.4, 135.9, 135.3, 133.0, 132.9, 132.8, 132.7, 132.6, 132.5, 132.0, 130.8, 130.3, 130.1, 129.5, 128.6, 128.5, 128.3, 126.8, 124.5, 120.3 (P*Ph*$_2$, C_6H$_4$CC, C_6H$_4$NC), 94.1, 89.5 (*C*≡*C*), 27.6, 27.4, 27.2, 27.0 (*C*H$_2$PPh$_2$). ^{31}P NMR ($CDCl_3$): δ 38.5 ($^1J_{WP} = 231$ Hz). IR (CH_2Cl_2, cm^{-1}): 2201 (m, ν_{CN}), 2008 (s, ν_{CO}), 1940 (s, ν_{CO}). Anal. Calc. for $C_{88}H_{64}Cl_2I_2N_2O_4P_4PdW_2 \cdot 0.5CH_2Cl_2$: C, 48.78; H, 3.01; N, 1.29. Found: C, 48.67; H, 2.73; N, 1.37%. mp 135–139 °C (dec.).

2.17. Synthesis of compound **24**

The synthesis follows the procedure described for **21**, using **10** and PtI_2. Orange-yellow micro-crystals. Yield: 30%. ^{1}H NMR ($CDCl_3$): δ 7.74–7.65 (8H, P*Ph*$_2$), 7.58 (d, $J = 8.6$ Hz, 2H, C_6H_4NC), 7.51 (d, $J = 8.6$ Hz, 2H, C_6H_4NC), 7.39–7.20 (12H, P*Ph*$_2$), 7.11 (d, $J = 8.3$ Hz, 2H, C_6H_4CC), 6.46 (d, $J = 8.3$ Hz, 2H, C_6H_4CC), 3.01–2.86 (m, 2H, CH_2PPh$_2$), 2.74–2.64 (m, 2H, CH_2PPh$_2$). ^{13}C{^{1}H} NMR ($CDCl_3$): δ 264.4 (W≡*C*), 212.3 (*C*O, $^1J_{PC}^{cis} = 7.0$ Hz, $^1J_{PC}^{trans} = 45.0$ Hz), 149.4, 135.8, 135.4, 134.0, 132.9, 132.7, 132.6, 132.5, 132.4, 132.2, 132.0, 131.1, 130.8, 130.5, 130.3, 130.2, 129.5, 129.4, 129.2, 128.8, 128.6, 128.5, 128.4, 128.3, 127.8, 126.9, 126.7, 124.8, 120.4 (P*Ph*$_2$, C_6H$_4$NC, C_6H$_4$CC), 94.1, 89.6 (*C*≡*C*), 27.4, 27.3, 27.2, 27.1 (*C*H$_2$PPh$_2$). ^{31}P NMR ($CDCl_3$): δ 38.5 ($^1J_{WP} = 231$ Hz). IR (CH_2Cl_2, cm^{-1}): 2197 (m, ν_{CN}), 2006 (s, ν_{CO}), 1942 (s, ν_{CO}). Anal. Calc. for $C_{88}H_{64}Cl_2I_2N_2O_4P_4PtW_2 \cdot 0.5CH_2Cl_2$: C, 46.88; H, 2.89; N, 1.24. Found: C, 46.77; H, 2.21; N, 1.45%. mp 147–150 °C (dec.).

2.18. Synthesis of compound **25**

Compound **11** (290 mg) was added to a suspension of PdI_2 (48 mg) in THF (30 mL). The mixture was stirred at r.t. overnight, followed by filtration. Then the solvent was removed in vacuo. The residue was washed with hexane, dried, and redissolved in CH_2Cl_2. After filtration, hexane was added to the solution to afford a yellow-orange crystalline solid. Yield: 32%. ^{1}H NMR ($CDCl_3$): δ 7.73–7.67 (8H, P*Ph*$_2$), 7.53 (d, $J = 8.4$ Hz, 2H, C_6H_4), 7.49 (d, $J = 8.4$ Hz, 2H, C_6H_4), 7.41–7.21 (14H, P*Ph*$_2$, C_6H_2i-Pr$_2$), 7.10 (d, $J = 8.3$ Hz, 2H, CC_6H_4), 6.46 (d, $J = 8.3$ Hz, 2H, CC_6H_4), 3.59–3.53 (m, 2H, C*H*(CH$_3$)$_2$), 2.98–2.89 (m, 2H, CH_2PPh$_2$), 2.70–2.61 (m, 2H, CH_2PPh$_2$), 1.36 (d, $J = 6.8$ Hz, 12H, CH_3). ^{13}C{^{1}H} NMR ($CDCl_3$): δ 264.9

(W≡*C*), 212.3 (*C*O, $^{1}J_{PC}^{cis} = 6.0$ Hz, $^{1}J_{PC}^{trans} = 46.0$ Hz), 148.9, 147.2, 135.8, 135.2, 132.9, 132.8, 132.7, 132.5, 132.1, 131.7, 131.5, 130.6, 130.3, 130.1, 129.4, 128.8, 128.6, 128.5, 127.0, 126.0, 123.7, 122.9, 122.3, 121.2 (P*Ph*$_2$, C*C*$_6$H$_4$CC, *C*$_6$H$_4$, *C*$_6$H$_2$*i*-Pr$_2$), 92.1, 91.9, 91.1, 90.5 (*C*≡*C*), 29.7 (*C*H(CH$_3$)$_2$), 27.5, 27.4, 27.1, 27.0 (*C*H$_2$PPh$_2$), 22.9 (*C*H$_3$). ^{31}P NMR (CDCl$_3$): δ 39.2 ($^{1}J_{WP} = 231$ Hz). IR (CH$_2$Cl$_2$, cm^{-1}): 2191 (m, ν_{CN}), 2008 (s, ν_{CO}), 1940 (s, ν_{CO}). mp 165–168 °C (dec.).

2.19. Synthesis of compound **26**

Compound **11** (290 mg) was added to a suspension of PtI$_2$ (60 mg) in THF (30 mL). The mixture was stirred at r.t. overnight, followed by filtration. Then the solvent was removed in vacuo. The residue was washed with hexane, dried, and redissolved in CH$_2$Cl$_2$. After filtration, hexane was added to the solution to afford a yellow-orange crystalline solid. Yield: 46%. ^{1}H NMR (CDCl$_3$): δ 7.75–7.66 (8H, P*Ph*$_2$), 7.54 (d, $J = 8.6$ Hz, 2H, C$_6$*H*$_4$), 7.50 (d, $J = 8.6$ Hz, 2H, C$_6$*H*$_4$), 7.40–7.20 (14H, P*Ph*$_2$, C$_6$*H*$_2$*i*-Pr$_2$), 7.10 (d, $J = 8.3$ Hz, 2H, CC$_6$*H*$_4$), 6.46 (d, $J = 8.3$ Hz, 2H, CC$_6$*H*$_4$), 3.61–3.47 (m, 2H, C*H*(CH$_3$)$_2$), 3.12–2.86 (m, 2H, C*H*$_2$PPh$_2$), 2.74–2.55 (m, 2H, C*H*$_2$PPh$_2$), 1.36 (d, 12H, C*H*$_3$). ^{13}C{^{1}H} NMR (CDCl$_3$): δ (signal for alkylidyne carbon atom not found) 212.3 (*C*O, $^{1}J_{PC}^{cis} = 6.0$ Hz, $^{1}J_{PC}^{trans} = 46.0$ Hz), 156.8, 148.9, 147.1, 135.8, 135.2, 133.8, 132.9, 132.8, 132.7, 132.5, 132.3, 132.1, 131.9, 131.7, 131.5, 130.9, 130.7, 130.6, 130.3, 130.1, 129.8, 129.7, 129.6, 129.4, 129.1, 129.0, 128.8, 128.6, 128.5, 128.3, 128.0, 127.3, 127.0, 126.0, 125.9, 123.7, 123.5, 122.8, 122.3, 122.2, 122.1, 121.8, 121.2, 119.7, 115.8, 106.1 (P*Ph*$_2$, C*C*$_6$H$_4$CC, *C*$_6$H$_4$, *C*$_6$H$_2$*i*-Pr$_2$), 92.1, 91.9, 91.1, 90.5 (*C*≡*C*), 29.6 (*C*H(CH$_3$)$_2$), 27.5, 27.4, 27.1, 27.0 (*C*H$_2$PPh$_2$), 22.8 (*C*H$_3$). ^{31}P NMR (CDCl$_3$): δ 39.2 ($^{1}J_{WP} = 231$ Hz). IR (CH$_2$Cl$_2$, cm^{-1}): 2187 (m, ν_{CN}), 2008 (s, ν_{CO}), 1940 (s, ν_{CO}). mp 168–171 °C (dec.).

2.20. Synthesis of compound **27**

Compound **12** (300 mg) was added to a suspension of PdI$_2$ (48 mg) in THF (30 mL). The mixture was stirred at r.t. overnight. After filtration, the solvent was removed in vacuo. The residue was washed with hexane, dried, and redissolved in CH$_2$Cl$_2$. After filtration, hexane was added to the solution to afford a yellow-orange crystalline solid. Yield: 0.157 g, 43%. ^{1}H NMR (CDCl$_3$): δ 7.75–7.66 (8H, P*Ph*$_2$), 7.58–7.20 (26H, P*Ph*$_2$, C$_6$*H*$_4$CC, C$_6$*H*$_2$*i*-Pr$_2$), 7.10 (d, $J = 8.3$ Hz, 2H, CC$_6$H$_4$), 6.46 (d, $J = 8.3$ Hz, 2H, CC$_6$*H*$_4$), 3.56 (hept, $J = 6.8$ Hz, 2H, C*H*CH$_3$), 3.01–2.58 (m, 2H, C*H*$_2$PPh$_2$), 1.37 (d, $J = 6.8$ Hz, 12H, C*H*$_3$). ^{13}C{^{1}H} NMR (CDCl$_3$): δ 265.0 (W≡*C*), 212.3 (*C*O, $^{1}J_{PC}^{trans} = 46.0$ Hz, $^{1}J_{PC}^{cis} = 7.0$ Hz), 149.0, 147.3, 135.9, 135.6, 133.0, 132.9, 132.7, 132.6, 132.4, 132.1, 131.8, 131.7, 131.5, 130.9, 130.6, 130.3, 130.1, 129.5, 129.3, 129.1, 128.9, 128.8, 128.6, 128.5, 128.4, 128.3, 127.1, 126.2, 123.6, 123.4, 123.0, 122.9, 122.6, 121.4 (C*C*$_6$H$_4$, *C*$_6$H$_4$CC, *C*$_6$H$_2$*i*-Pr$_2$), 92.0, 91.9, 91.4, 91.3, 91.0, 90.5 (*C*≡*C*), 29.7 (*C*HCH$_3$), 27.5, 27.4, 27.3, 27.2 (*C*H$_2$PPh$_2$), 22.9 (*C*H$_3$). ^{31}P NMR (CDCl$_3$): δ 39.2 ($^{1}J_{WP} = 231$ Hz). IR (CH$_2$Cl$_2$, cm^{-1}): 2193 (m, ν_{CN}), 2008 (s, ν_{CO}), 1940 (s, ν_{CO}). mp 170–173 °C (dec.).

2.21. Synthesis of compound **28**

Compound **12** (290 mg) was added to a suspension of PtI$_2$ (60 mg) in THF (30 mL). The mixture was stirred at r.t. overnight, followed by filtration. The solvent was removed in vacuo. The residue was washed with hexane, dried, and redissolved in CH$_2$Cl$_2$. After filtration, hexane was added to the solution to afford a yellow-orange crystalline solid. Yield: 0.22 g, 64%. ^{1}H NMR (CDCl$_3$): δ 7.75–7.66 (8H, P*Ph*$_2$), 7.60–7.20 (26H, P*Ph*$_2$, C$_6$*H*$_4$CC, C$_6$*H*$_2$*i*-Pr$_2$), 7.10 (d, $J = 8.3$ Hz, 2H, CC$_6$*H*$_4$), 6.46 (d, $J = 8.3$ Hz, 2H, CC$_6$*H*$_4$), 3.57 (hept, $J = 6.8$ Hz, 2H, C*H*CH$_3$), 3.01–2.84 (m, 2H, C*H*$_2$PPh$_2$), 2.75–2.58 (m, 2H, C*H*$_2$PPh$_2$), 1.37 (d, $J = 6.8$ Hz, 12H, C*H*$_3$). ^{13}C{^{1}H} NMR (CDCl$_3$): δ (signals for alkylidyne and carbonyl carbon atoms not found) 147.2, 135.9, 135.3, 133.0, 132.9, 132.8, 132.7, 132.6, 132.5, 132.1, 131.7, 131.6, 131.5, 130.6, 130.4, 130.3, 130.1, 129.4, 128.6, 128.5, 127.1, 125.9, 123.5, 123.3, 122.8, 122.5, 121.3 (C*C*$_6$H$_4$, *C*$_6$H$_4$CC, *C*$_6$H$_2$*i*-Pr$_2$), 91.9, 91.8, 91.4, 91.3, 90.9, 90.6 (*C*≡*C*), 29.6, 27.6, 27.4 (*C*H$_2$PPh$_2$), 22.8 (*C*H$_3$). ^{31}P NMR (CDCl$_3$): δ 38.5 ($^{1}J_{WP} = 231$ Hz). IR (CH$_2$Cl$_2$, cm^{-1}): 2187 (m, ν_{CN}), 2008 (s, ν_{CO}), 1940 (s, ν_{CO}). mp 170–173 °C (dec.).

2.22. Synthesis of compound **29**

The synthesis follows the procedure described for **13**, whereby 2,6-diisopropylisocyanobenzene was used. White crystals. Yield: 30%. ^{1}H NMR (CDCl$_3$): δ 7.31 (m, 1H, C$_6$*H*$_3$NC), 7.18 (d, $J = 7.7$ Hz, 2H, C$_6$*H*$_3$NC), 3.26 (hept, $J = 6.9$ Hz, 2H, C*H*Me$_2$), 1.32 (d, $J = 6.9$ Hz, 12H, C*H*$_3$). ^{13}C{^{1}H} NMR (CDCl$_3$): δ 216.8, 214.5 (*C*O), 144.9, 129.1, 123.5 (*C*$_6$H$_3$NC), 30.2 (*C*HMe$_2$), 22.4 (*C*H$_3$). IR (CH$_2$Cl$_2$, cm^{-1}): 2141 (w, ν_{CN}), 2058 (m, ν_{CO}), 1956 (s, ν_{CO}).

2.23. Synthesis of compound **30**

The synthesis follows the procedure described for **14**, whereby 2,6-diisopropylisocyanobenzene was used. White crystals. Yield: 40%. ^{1}H NMR (CDCl$_3$): δ 7.36 (m, 1H, C$_6$*H*$_3$NC), 7.20 (d, $J = 7.8$ Hz, 2H, C$_6$*H*$_3$NC), 3.38 (hept, $J = 6.9$ Hz, 2H, C*H*Me$_2$), 1.30 (d, $J = 6.9$ Hz, 12H, C*H*$_3$). ^{13}C{^{1}H} NMR (CDCl$_3$): δ 186.9, 184.1 (*C*O), 145.9, 130.2, 123.6 (*C*$_6$H$_3$NC), 30.1 (*C*HMe$_2$), 22.5 (*C*H$_3$). IR (CH$_2$Cl$_2$, cm^{-1}): 2185 (w, ν_{CN}), 2154 (w, ν_{CN}), 2039 (m, ν_{CO}), 1989 (s, ν_{CO}), 1931 (s, ν_{CO}).

2.24. Synthesis of compound **31**

To a suspension of PdCl$_2$ (0.25 g) in THF (30 mL), 2,6-*i*-Pr$_2$C$_6$H$_3$NC (0.82 g) was added. The mixture was stirred at

r.t. overnight, followed by filtration. Then the solvent was removed in vacuo. The residue was washed with hexane, dried, and redissolved in CH_2Cl_2. After filtration, hexane was added to the solution to afford yellow micro-crystals. Yield: 50%. ^{1}H NMR ($CDCl_3$): δ 7.61–7.36 (1H, C_6H_3NC), 7.27–7.21 (2H, C_6H_3NC), 3.36 (hept, $J = 6.9$ Hz, 2H, $CHCH_3$), 13.2 (d, $J = 6.9$ Hz, 12H, CH_3). $^{13}C\{^1H\}$ NMR ($CDCl_3$): δ 146.7, 146.4, 131.7, 131.4, 124.0, 123.7 (C_6H_3NC), 29.8 ($CHCH_3$), 22.7 (CH_3). IR (CH_2Cl_2, cm^{-1}): 2224 (s, ν_{CN}), 2210 (s, ν_{CN}).

2.25. Synthesis of compound 32

The synthesis follows the procedure described for **17**, whereby 2,6-diisopropylisocyanobenzene was used. Yellow-orange cyrstals. Yield: 75%. ^{1}H NMR ($CDCl_3$): δ 7.41 (m, 1H, C_6H_3NC), 7.23 (d, $J = 7.8$ Hz, 2H, C_6H_3NC), 3.56 (hept, $J = 6.8$ Hz, 2H, $CHMe_2$), 1.34 (d, $J = 6.8$ Hz, 12H, CH_3). $^{13}C\{^1H\}$ NMR ($CDCl_3$): δ 146.9, 131.1, 123.7 (C_6H_3NC), 29.6 ($CHMe_2$), 23.0 (CH_3). IR (CH_2Cl_2, cm^{-1}): 2197 (s, ν_{CN}).

2.26. Synthesis of compound 33

The synthesis follows the procedure described for **18**, whereby 2,6-diisopropylisocyanobenzene was used. Dull yellow cyrstals. Yield: 55%. ^{1}H NMR ($CDCl_3$): δ 7.41 (m, 1H, C_6H_3NC), 7.23 (d, $J = 7.8$ Hz, 2H, C_6H_3NC), 3.56 (hept, $J = 6.8$ Hz, 2H, $CHMe_2$), 1.34 (d, $J = 6.8$ Hz, 12H, CH_3). $^{13}C\{^1H\}$ NMR ($CDCl_3$): δ 146.9, 131.0, 123.7 (C_6H_3NC), 29.6 ($CHMe_2$), 23.0 (CH_3). IR (CH_2Cl_2, cm^{-1}): 2193 (s, ν_{CN}).

2.27. Synthesis of compound 34

Compound **4** (0.15 g) was added to a suspension of PdI_2 (0.10 g) in THF (30 mL). The mixture was stirred at r.t. for 2 h, followed by filtration. Then the solvent was removed in vacuo. The residue was washed with hexane, dried, and redissolved in CH_2Cl_2. After filtration, hexane was added to the solution to afford an orange crystalline solid. Yield: 0.1 g, 46%. ^{1}H NMR ($CDCl_3$): δ 7.54 (s, 4H, C_6H_4CC), 7.49 (s, 4H, C_6H_4CC), 7.38 (s, 2H, C_6H_2i-Pr_2), 3.56 (m, 2H, $CHCH_3$), 3.19 (s, 1H, CCH), 1.37 (d, $J = 6.8$ Hz, 12H, CH_3). $^{13}C\{^1H\}$ NMR ($CDCl_3$): δ 147.2, 132.1, 131.7, 131.5, 127.1, 126.0, 123.4, 122.9, 122.5, 122.2 (C_6H_4CC, C_6H_2i-Pr_2), 91.8, 91.1, 90.7, 90.5 ($C{\equiv}C$), 83.2 (CCH), 79.1 (CCH). IR (CH_2Cl_2, cm^{-1}): 2193 (s, ν_{CN}). mp 185–188 °C (dec.).

2.28. X-ray crystal structure analysis of complex 17

The crystal parameters of compound **17** and information on data collection and refinement are summarized in Table 1. The diffraction data were collected on a Rigaku AFC7R diffractometer with graphite-monochromatized Mo Kα X-ray radiation ($\lambda = 0.71073$ Å). Empirical absorption corrections based on the ψ-scan of four strong reflections was applied. The centric space group was based on statistical analysis of intensity distribution and confirmed by the successful refinement of the structure solved by direct methods (SIR-92 [21]) and expanded by Fourier methods and refined by full-matrix least-squares using the software package TEXSAN [22]. The least squares refinements were on F using reflections with $I > 3\sigma(I)$. Hydrogen atoms at calculated positions with thermal parameters equal to 1.3 times that of the attached C atoms were included in the calculations, but not refined.

Table 1
Crystal and data collection parameters for complex **17**

Formula	$W_2I_2PdCl_2O_4N_6C_{32}H_{40}$
Formula weight	1371.52
Crystal system	Triclinic
Space group	$P\bar{1}$ (No. 2)
a (Å)	11.934(3)
b (Å)	26.196(3)
c (Å)	7.452(2)
α (°)	97.46(2)
β (°)	105.19(2)
γ (°)	78.40(2)
V (Å^3)	105.19(2)
Z	2
D_{cal} (g cm^{-3})	2.075
μ (cm^{-1})	72.07
$F(000)$	1280
T (K)	301
Crystal color	Red
Crystal dimensions (mm^3)	$0.20 \times 0.15 \times 0.30$
Total reflections measured	6053
Unique reflections	5721
R	0.035
R_w	0.044
Goodness-of-fit	1.74
Maximum Δ/σ	0.04
Maximum peak in final Fourier map (e Å^{-3})	1.08
Minimum peak in final Fourier map (e Å^{-3})	−0.68

3. Results and discussion

3.1. Synthesis of the metal complexes

The synthesis of the tungsten complexes **7**–**11**, which contain unsaturated alkylidyne ligands with free terminal isocyano groups, has previously been described [17]. Complex **12** was prepared by a similar procedure, as shown in Schemes 1 and 2. The heteronuclear metal complexes **13**–**28** were prepared by reaction of the respective isocyano-terminated alkylidyne tungsten complexes **7**–**12** with the metal complex reagents $Cr(CO)_5(THF)$ (**13**), $ReCl(CO)_3(THF)_2$ (**14**, **19**, **22**), $ReBr(CO)_3(THF)_2$ (**15**), $PdCl_2$ (**16**), PdI_2 (**17**, **20**, **23**, **25**, **27**), and PtI_2 (**18**, **21**, **24**, **26**, **28**) in THF or dichloromethane solution (see Scheme 3). The compounds were recrystallized from dichloromethane and hexane. The simple isocyanide metal complexes **29**–**33** were prepared from the same metal complex fragments and 2,6-diisopropylphenylisocyanide under similar conditions. The combination of PdI_2 and isocyanide **4** afforded complex **34**.

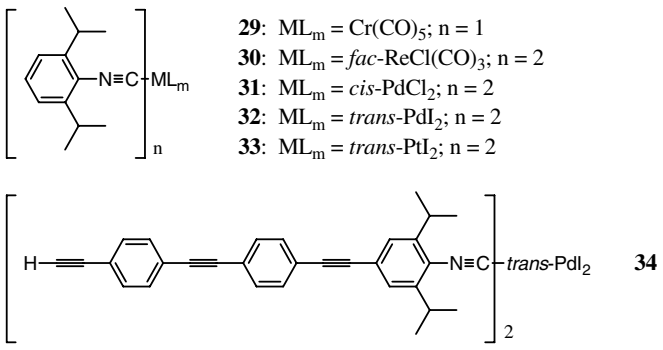

3.2. Crystal structure analysis of complex 17

The crystal structure of complex **17** was determined by X-ray crystallography. The structure contains two independent molecules with similar metric parameters. Selected bond lengths and bond angles for one of the molecules are listed in Table 2. Fig. 1 shows a drawing of that molecule. The structure confirms the linear geometry of the diiodo-bis-(isocyanide)palladium unit. The strict linearity of the central C(10)–Pd(1)–C(10*) fragment is imposed crystallographically. The Pd(1)–C(10)–N(3) and C(10)–N(3)–C(7) angles deviate from linearity by only 3°. The angle on the alkylidyne carbon atom, W(1)–C(3)–C(4), is 170°. This deviation from linearity is not larger than observed for several other benzylidyne metal complexes [23]. All bond lengths are within the expected ranges.

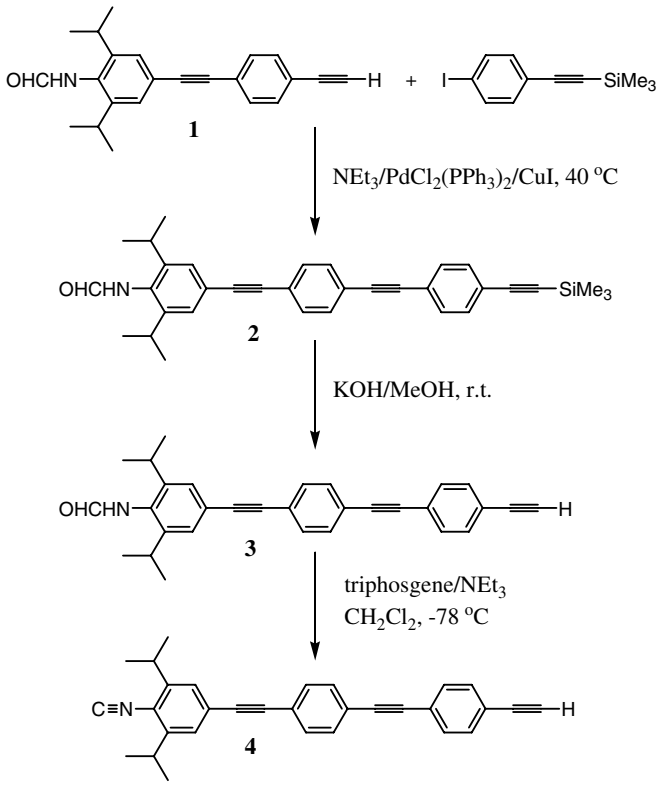

Scheme 1.

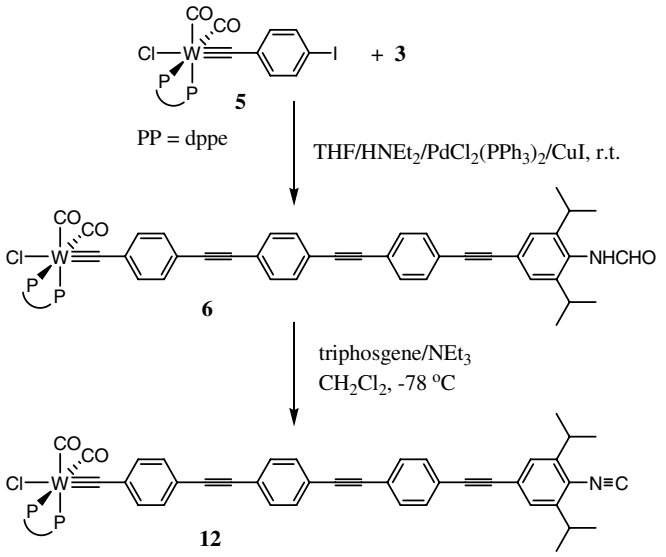

Scheme 2.

3.3. Bonding in alkylidyne metal complexes

Alkylidyne metal complexes have been the subject of several theoretical studies [24]. For octahedral systems, the qualitative bonding description is straightforward due to the clean separation of the metal–ligand σ and π bonds. As shown in Fig. 2, the alkylidyne ligand forms two π bonds with the metal center, involving the metal d_{xz} and d_{yz} orbitals. In metal–benzylidyne systems the two π bonds are not degenerate. In the free benzylidyne ligand, the out-of-plane p orbital of the alkylidyne carbon atom, i.e., the orbital conjugated with the phenyl π system, is about 42 kJ/mol lower in energy than the in-plane p orbital. In the metal–carbon triple bond, this splitting is diminished in the M–C π orbitals, but enlarged in the M–C π* orbitals. The equatorial metal d_{xy} orbital is nonbonding with respect to the metal–carbon triple bond. This orbital is stabilized by interaction with a suitable combination of carbonyl π* orbitals. According to the calculations, the energy of the d_{xy} orbital is below the energy of the halogen p orbitals in the tetracarbonyl complexes $M(CR)X(CO)_4$ (M = Cr, Mo, W; X = Cl, Br, I). However, in the dicarbonyl complexes of the type $M(CR)X(CO)_2L_2$ (L = donor ligand), e.g., those studied here, the d_{xy} orbital is probably the HOMO, at least for X = Cl and Br. This assessment is supported by the observation that the nature of the halide ligand exerts only a minor influence on the absorption as well as emission properties [9c]. The carbonyl π* orbitals oriented along the z direction are essentially nonbonding since the M–C π orbitals are much lower in energy. Thus, we may use the simplified molecular orbital scheme shown in Fig. 2 as a basis for our discussion.

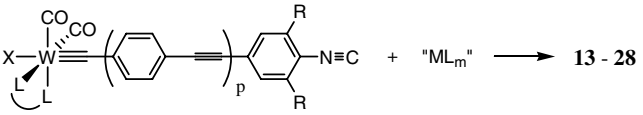

7: X = Cl; LL = TMEDA; R = H; p = 0
8: X = Br; LL = TMEDA; R = H; p = 0
9: X = Cl; LL = dppe; R = H; p = 0
10: X = Cl; LL = dppe; R = H; p = 1
11: X = Cl; LL = dppe; R = isopropyl; p = 2
12: X = Cl; LL = dppe; R = isopropyl; p = 3

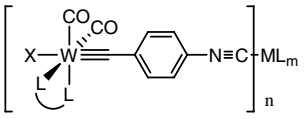

13: X = Cl; LL = TMEDA; n = 1; $ML_m = Cr(CO)_5$
14: X = Cl; LL = TMEDA; n = 2; ML_m = *fac*-$ReCl(CO)_3$
15: X = Br; LL = TMEDA; n = 2; ML_m = *fac*-$ReBr(CO)_3$
16: X = Cl; LL = TMEDA; n = 2; ML_m = *cis*-$PdCl_2$
17: X = Cl; LL = TMEDA; n = 2; ML_m = *trans*-PdI_2
18: X = Cl; LL = TMEDA; n = 2; ML_m = *trans*-PtI_2
19: X = Cl; LL = dppe; n = 2; ML_m = *fac*-$ReCl(CO)_3$
20: X = Cl; LL = dppe; n = 2; ML_m = *trans*-PdI_2
21: X = Cl; LL = dppe; n = 2; ML_m = *trans*-PtI_2

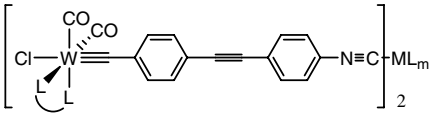

22: LL = dppe; ML_m = *fac*-$ReCl(CO)_3$
23: LL = dppe; ML_m = *trans*-PdI_2
24: LL = dppe; ML_m = *trans*-PtI_2

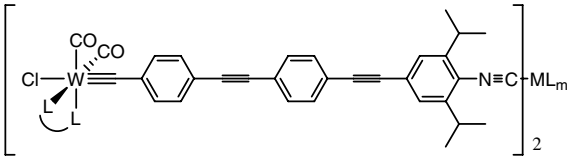

25: LL = dppe; ML_m = *trans*-PdI_2
26: LL = dppe; ML_m = *trans*-PtI_2

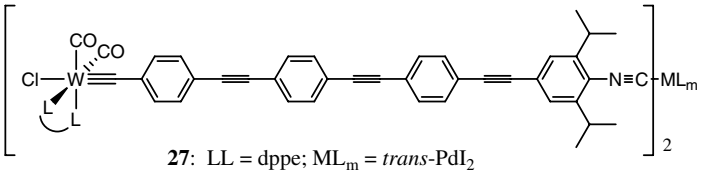

27: LL = dppe; ML_m = *trans*-PdI_2
28: LL = dppe; ML_m = *trans*-PtI_2

Scheme 3.

Table 2
Selected bond lengths (Å) and bond angles (°) for complex **17**

Bond lengths (Å)		Bond angles (°)	
W(1)–C(3)	1.79(1)	W(1)–C(3)–C(4)	170(1)
W(1)–C(1)	1.96(2)	Cl(1)–W(1)–C(3)	169.3(4)
W(1)–C(2)	2.00(1)	C(1)–W(1)–C(2)	87.9(6)
W(1)–N(1)	2.291(9)	C(1)–W(1)–N(2)	95.5(5)
W(1)–N(2)	2.296(8)	N(1)–W(1)–N(2)	78.8(3)
W(1)–Cl(1)	2.557(3)	C(2)–W(1)–N(1)	97.3(5)
C(3)–C(4)	1.47(2)	C(7)–N(3)–C(10)	177(1)
C(7)–N(3)	1.42(1)	N(3)–C(10)–Pd(1)	177(1)
N(3)–C(10)	1.15(1)	Cl(1)–W(1)–C(1)	87.3(5)
C(10)–Pd(1)	1.96(1)	Cl(1)–W(1)–C(2)	85.9(4)
Pd(1)–I(1)	2.582(1)	Cl(1)–W(1)–N(1)	87.3(3)
		Cl(1)–W(1)–N(2)	88.6(2)
		C(10)–Pd(1)–I(1)	91.6(4)
		C(10)–Pd(1)–C(10*)	180

3.4. IR spectroscopic data of the metal complexes

Relevant IR data are collected in Table 3. In isocyanide metal complexes, the C–N stretching frequency is a sensitive probe for the electron density of the metal center. In general, the C–N stretch shifts to higher frequencies with increasing electron acceptor ability of the metal complex fragment [10]. In the series **13**–**18**, the increase of the C–N stretching frequency from the free isocyanide **7** (2124 cm^{-1}) is 13 wavenumbers for $Cr(CO)_5$, 43 for $ReX(CO)_3$ (X = Cl, Br), 69 for *trans*-PtI_2, 75 for *trans*-PdI_2, and 104 for *cis*-$PdCl_2$. Thus, the IR data indicate that the palladium metal complex fragments are the strongest electron acceptors in this series.

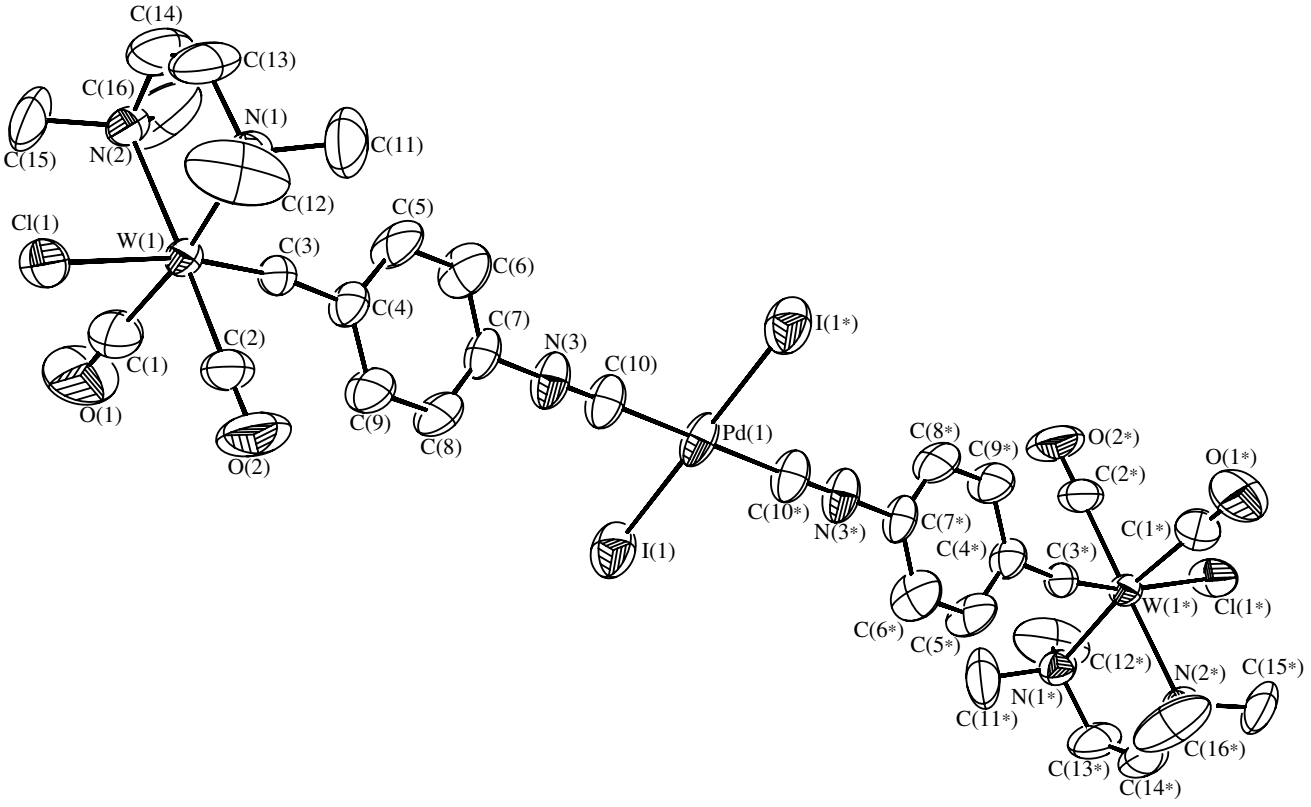

Fig. 1. Molecular structure of compound **17**. The thermal ellipsoids are shown at the 40% probability level.

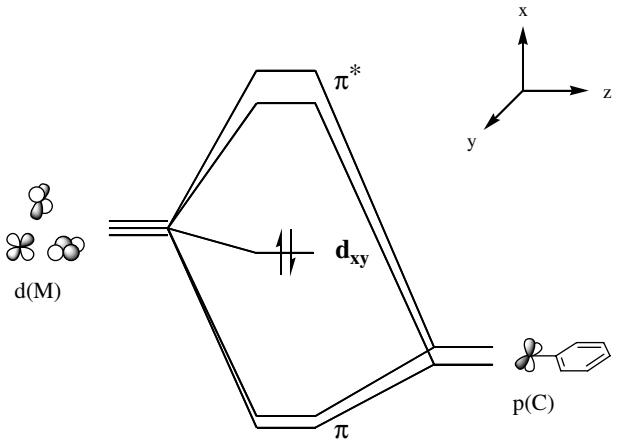

Fig. 2. Simplified molecular orbital scheme for a metal benzylidyne complex.

Table 3
IR and ^{13}C NMR spectroscopic data of selected compounds

Complex	ν(CO) (cm^{-1})	ν(CN) (cm^{-1})	δ(W≡*C*–) (ppm)	δ(W–*C*O) (ppm)
7	1992, 1902	2124	257.5	220.5
9	2010, 1944	2124	261.7	212.0
10	2006, 1940	2125	264.6	212.3
11	2008, 1940	2120	265.0	212.3
12	2008, 1940	2116	265.0	212.3
13	1990, 1902	2137	257.3	220.4
14	1992, 1904	2185, 2151	257.5	221.5
16	1994, 1906	2228, 2212	256.3	221.4
17	1992, 1906	2199	256.0	220.2
18	1994, 1904	2193	256.1	220.2
19	2012, 1944	2185, 2149	260.6	211.9
20	2014, 1946	2199	260.0	211.8
21	2014, 1946	2191	260.1	211.8
22	2008, 1940	2185, 2149	264.5	211.9
23	2008, 1940	2201	264.5	212.2
24	2006, 1942	2197	264.4	212.3
25	2008, 1940	2191	264.9	212.3
26	2008, 1940	2187	–	212.3
27	2008, 1940	2193	265.0	212.3
28	2008, 1940	2187	–	–

The carbonyl stretching frequencies of the $W(CO)_2$ fragment are only marginally affected by the nature of the metal complex fragment coordinated to the isocyanide group. For example, even though the isocyanide stretching frequency of **7** increases by 104 cm^{-1} upon coordination to $PdCl_2$, the concomitant change of the carbonyl stretching frequencies for the $W(CO)_2$ fragment is only 4 cm^{-1}. Considering that the π bond between the carbonyl ligands and the metal center involves primarily the d_{xy} orbital, which is orthogonal to the metal–carbon triple bond, this is not an unexpected observation. In contrast, replacement of the equatorial tmeda (tetramethylethylenediamine) ligand by dppe [bis(diphenylphosphino)ethane] causes the carbonyl stretching frequencies to shift to higher energies by about

20–30 wavenumbers. Evidently, the orthogonality of the d_{xy} orbital and the metal–carbon π bonds insulates the d_{xy} orbital from modifications of the extended benzylidyne π system. Conversely, the energy of the d_{xy} orbital may be changed without significantly perturbing the metal–benzylidyne π system.

3.5. NMR spectroscopic data of the metal complexes

Relevant NMR data are collected in Table 3 and plotted in Fig. 3. Even though the ^{13}C NMR signals of the alkylidyne carbon atoms of all complexes fall within the narrow range of δ 256–265, the chemical shift parameter is of diagnostic value. Replacement of the tmeda ligand by dppe causes the signal to shift downfield by about 4 ppm, e.g., from 257.5 to 261.7 ppm for complexes **7** and **9**. Extension of the benzylidyne ligand by one phenyleneethynylene unit, on going from **9** to **10**, results in a downfield shift of 2.9 ppm. Insertion of a second phenyleneethynylene group, changing **10** to **11**, causes a further downfield shift of 0.4 ppm, while the influence of a third phenyleneethynylene group, on going from **11** to **12**, can barely be discerned. Within the two series of phenylene-bridged complexes that are based on the parents **7** and **9** the isocyanide-coordinated metal complex fragments of **13**–**18** and **19**–**21** cause upfield shifts of the alkylidyne carbon signals of up to 1.6 ppm, roughly mirroring the relative electron acceptor abilities of the metal centers. Insertion of the phenyleneethynylene groups greatly diminishes the influence of the isocyanide-coordinated metal centers on the chemical shift of the alkylidyne carbon atom.

The individual factors contributing to these changes in chemical shift have not been identified. However, the downfield shift of the resonance of the alkylidyne carbon atom upon insertion of phenyleneethynylene units may be correlated with the extension of the π system of the alkylidyne ligands. ^{13}C NMR chemical shifts generally shift towards lower field when the electronic excitation energy decreases [25].

The ^{13}C and ^{31}P NMR signals of the carbonyl carbon and dppe phosphorus atoms of the tungsten alkylidyne fragments are nearly unaffected by the various modifications of the alkylidyne ligands.

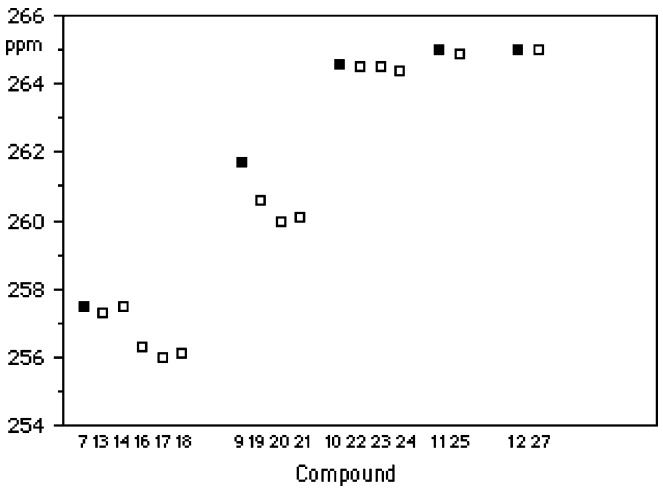

Fig. 3. Plot of the ^{13}C NMR chemical shifts of the benzylidyne carbon atoms of selected compounds.

3.6. Electronic absorption spectra of the metal complexes

The results of the photophysical measurements are summarized in Table 4. Fig. 4a shows the absorption and emission spectra of complex **18** as a representative example. The electronic absorption and emission energies of selected complexes are plotted in Fig. 5. The spectra of all compounds feature two low-energy absorptions. A band of low intensity ($\varepsilon \leqslant 10^3\ M^{-1}\ cm^{-1}$) in the 450–500 nm range is assigned to the $d \rightarrow \pi^*$ transition, while a band in the 340–380 nm range ($\varepsilon = 10^4$–$10^5\ M^{-1}\ cm^{-1}$) is assigned to the $\pi \rightarrow \pi^*$ transition [9c]. Replacement of the tmeda ligand in **7** by the less strongly donating (and weakly π backbonding) dppe ligand in **9** lowers the energy of the d_{xy} orbital. Consequently, the $d \rightarrow \pi^*$ transition occurs at higher energy in **9** than in **7**, by 932 cm^{-1}. At the same time the energy of the $\pi \rightarrow \pi^*$ transition is less affected, with the $\pi \rightarrow \pi^*$ transition energy of **9** being lower than that of **7** by 499 cm^{-1}. Replacement of the chloro ligand of **7** by bromide to afford **8** does not noticeably influence the energies of the $d \rightarrow \pi^*$ and $\pi \rightarrow \pi^*$ transitions. The lack of influence of the halide ligands on the electronic spectra of metal alkylidynes has been noted earlier [9c]. A decrease in the energy of the $\pi \rightarrow \pi^*$ transition in the series **9**–**12** is observed, probably due to the extension of the benzylidyne ligand by phenyleneethynylene groups which would cause a narrowing of the $\pi \rightarrow \pi^*$ gap. This effect appears to have leveled off after insertion of two phenyleneethynylene units. The fact that in the same series the energy of the $d \rightarrow \pi^*$ transition is dropping considerably less than half of the decrease of the $\pi \rightarrow \pi^*$ transition energy suggests that the extension of the π system raises the energy of the π orbitals more than it lowers the energy of the π^* orbitals. The $\pi \rightarrow \pi^*$ absorption of the rhenium complexes **14** and **15** is split into two peaks, separated by about 1200 cm^{-1}. The origin of this feature may be vibronic coupling with the arene ring [9a] that is enhanced by the *cis*-arrangement of the areneisocyanide groups on the rhenium center.

In the phenylene-bridged series **7**/**13**–**18** and **9**/**19**–**21**, the isocyanide-coordinated metal center exerts a pronounced influence on the electronic absorption energies. The addition of metal centers to the isocyanide group lowers the energy of the $\pi \rightarrow \pi^*$ transition. Two factors appear to be at play here, the generic extension of the π system by an additional metal–carbon bond and the specific influence of the metal complex fragment. The latter factor may account for the strikingly low $\pi \rightarrow \pi^*$ transition energies of complexes **13** and **14**. The metal centers in the $Cr(CO)_5$ and $ReCl(CO)_3$ fragments have a d^6 electron configuration and are consequently potential π donors. Thus, π donation

Table 4
Electronic absorption and emission data of the metal alkylidyne complexes in CH_2Cl_2 (λ/nm, ε/$M^{-1}cm^{-1}$)

Complex	$\pi \rightarrow \pi^*$/nm (ε/M^{-1} cm^{-1})	$d \rightarrow \pi^*$/nm (ε/M^{-1} cm^{-1})	Emission/nm Emission lifetime	Quantum yield $\Phi_{em} \times 10^4$	Radiative decay rate constant/s^{-1}, Φ_{em}/τ
7	344 (19000)	476 (560)	656, 700 (sh)[a]	16.0	
			$\tau = 0.45$ μs	11.1[a]	2.5×10^3[a]
8	344 (18900) 476 (600)				
9	350 (20700) 360 (sh)	456 (590)	664, 698 (sh)[a] $\tau = 0.15$ μs		
10	374 (37600) 388 (sh)	462 (950)	667, 700 (sh) $\tau = 0.69$ μs	7.2	1.0×10^3
11	382 (69400) 398 (sh)	460 (1650)	670 $\tau = 0.86$ μs	3.0	3.5×10^2
12	346 (sh) 380 (84700) 404 (sh)	462 (1690)	670 $\tau = 0.87$ μs	3.4	3.9×10^2
13	368 (sh) 382 (20000)	480 (940)	662[a] $\tau = 0.47$ μs		
14	374 (63800), 358 (65100)	490 (1640)	665, 690 (sh)[a] $\tau = 0.32$ μs	19.1 13.6[a]	4.3×10^3[a]
15	376 (66900), 358 (69200)	488 (2050)			
16	358 (54600)	500 (1640)	ND	NE	
17	362 (71900)	494 (1900)	ND	NE	
18	372 (68900)	500 (1760)	670, 700 (sh) $\tau = 0.22$ μs	14.7	6.7×10^3
19	364 (52500) 382 (52000)	474 (1240)	662, 693 (sh) $\tau = 0.14$ μs		
20	366 (61900) 378 (sh)	484 (1490)	ND		
21	380 (59000)	480 (1650)	671, 700 (sh) $\tau = 0.10$ μs		
22	380 (109900) 400 (sh)	464 (2980)	668, 703 (sh) $\tau = 0.64$ μs	6.5	2.0×10^3
23	380 (106600) 400 (sh)	470 (3050)	670, 704 (sh) $\tau = 0.12$ μs[b]	0.6	0.4×10^3
24	384 (109000) 404 (sh)	470 (3130)	670, 704 (sh) $\tau = 0.63$ μs	6.4	1.0×10^3
25	340 (sh) 384 (152700) 404 (sh)	464 (3400, sh)	670 $\tau = 0.50$ μs	1.7	3.5×10^2
26	384 (161800) 404 (sh)	462 (3420, sh)	670 $\tau = 0.92$ μs	3.4	3.7×10^2
27	340 (sh) 380 (187300) 406 (sh)	466 (3240, sh)	670 $\tau = 0.80$ μs	3.3	4.2×10^2
28	360 (sh) 382 (23200) 406 (sh)	466 (3590, sh)	670 $\tau = 0.87$ μs	3.5	4.1×10^2

sh = shoulder. NE = non-emissive. ND = not detected.
[a] Measured in acetonitrile solution.
[b] Emission intensity is too weak to give reliable τ.

of electron density from these metal centers may decrease the gap between the π and π* orbitals by raising the energy of the π orbitals. The $d \rightarrow \pi^*$ transition is also affected by the addition of the isocyanide metal centers, but less so than the $\pi \rightarrow \pi^*$ transition. The $d \rightarrow \pi^*$ transition moves to lower energy as the electron-acceptor ability of the metal center increases. The change appears to be correlated directly with the electron acceptor ability of the isocyanide metal complex fragment, reflecting the trend indicated by the CN-stretching frequencies. The influence of the isocyanide-coordinated metal centers on the $d \rightarrow \pi^*$ and $\pi \rightarrow \pi^*$ transitions is still clearly discernible in the series **10/22**–**24**, but barely so in the more extended series **11/25**, **26** and **12/27**, **28**.

The 2,6-diisopropylphenylisocyanide complexes **29**–**33** serve as models for the local isocyanide metal complex fragments of the respective compounds **13**–**28**. The absorption spectra of compounds **31**, **32**, and **33** are shown in Fig. 4b. Relevant spectroscopic data are collected in Table 5. Complexes **29**–**33** exhibit only weak absorptions in the 325–400 nm range and, with the exception of **32**, no absorptions with wavelengths longer than 400 nm.

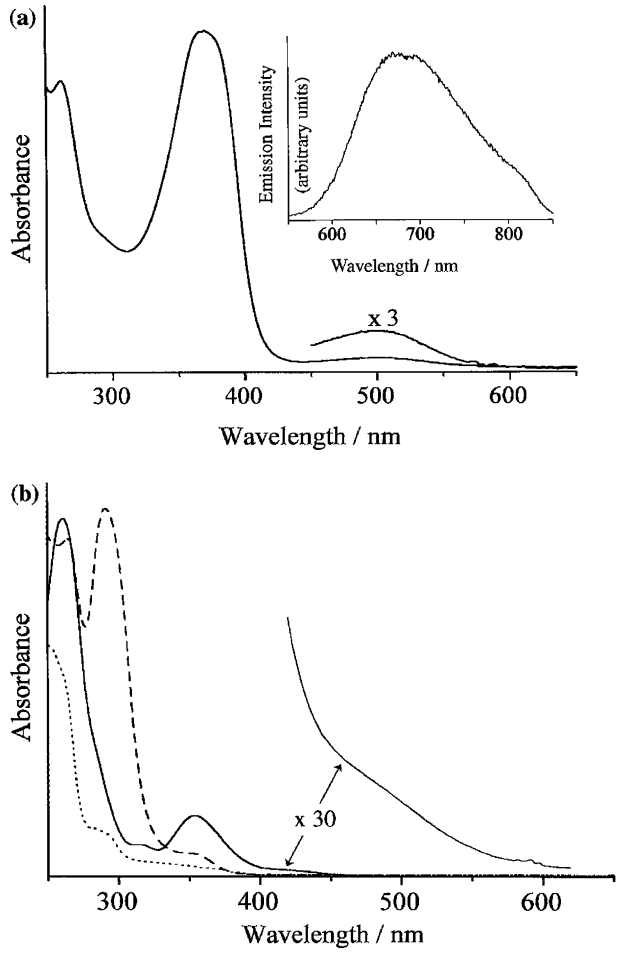

Fig. 4. (a) Electronic absorption and emission (inset) spectra of compound **18** in CH_2Cl_2 solution. (b) Electronic absorption spectra of compounds **31** (·····), **32** (——), and **33** (------) in CH_2Cl_2 solution. The absorption tail of **32** is enlarged.

Complex **32** features a long absorption tail of low intensity in the region of 400–600 nm. Consequently, the higher-energy features of all complexes **13**–**28** are dominated by the $\pi \rightarrow \pi^*$ transitions of the extended alkylidyne fragments, and the $d \rightarrow \pi^*$ transitions of the complexes containing $Cr(CO)_5$–, $ReX(CO)_3$–, $PdCl_2$–, and PtI_2–isocyanide metal complex fragments originate exclusively from the alkylidyne tungsten fragments. Only in the PdI_2-containing complexes **17**, **20**, **23**, **25**, and **27**, there is a small contribution from the palladium isocyanide fragment to the low-energy absorption.

3.7. Emission properties of the metal complexes

The emission data of the metal complexes are summarized in Table 4. The emission energies and emission lifetimes are plotted in Fig. 5b. All complexes except **16**, **17**, and **20** are emissive in fluid solution at room temperature. The maxima of the emission bands occur in the narrow range between 656 and 671 nm. So neither the substitution of tmeda by dppe on tungsten, nor the attachment of a metal center to the isocyanide group, nor the extension of the unsaturated alkylidyne ligand exert a significant influence on the emission energy. These observations suggest that the original excited state relaxes into a long-lived triplet excited state which is very similar for all compounds, and that the excited electron is not extensively delocalized over the extended π system. The large Stoke's shift of the emission, about 6300 cm^{-1}, may imply a significant change of the molecular geometry in the triplet excited state. One of the possibilities is bending of the alkylidyne ligand, e.g., as in **A**. In that case, the excited electron could remain localized on the alkylidyne carbon atom in an orbital of the bent metal alkylidyne unit. Experimental support for this kind of excited-state structure comes from the observation of facile protonation of alkylidyne ligands under irradiation [9b]. Other experiments suggest that in carbonylmetal alkylidyne systems the initial excited state rearranges into a metal ketenyl species **B** by forming a bond between the alkylidyne ligand and a carbonyl ligand. Supporting evidence for structure **B** derives from the observation that the excited states of alkylidyne carbonyltungsten complexes can be trapped as ketenyl derivatives by nucleophiles [26] or as oxyacetylene species by electrophiles [27]. In **B** the excited electron would most likely be associated with the newly formed carbon–carbon linkage. However, the Stoke's shift may also be explained by a bond length change of the metal–carbon triple bond [9a] or simply the electronic difference between the initial singlet excited state and the triplet character of the emissive state [9f].

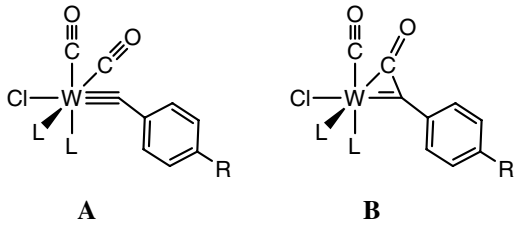

In contrast to the emission energies, the excited state lifetimes show a distinct dependence on the various molecular components (Table 4 and Fig. 5b). Replacement of tmeda in **7** by dppe to afford **9** shortens the lifetime by a small amount. There also appears to be a trend towards shorter lifetimes as electron-withdrawing metal centers are attached to the isocyanide group. The value of the emission lifetime of the platinum complex **26** is an exception to this trend. Considering the internal consistency of all other data, it is likely that the slight elevation of this value is due to some unknown experimental error. Most interestingly, the $PdCl_2$- and PdI_2-containing complexes **16**, **17** and **20** do not emit at all, and the emission of the extended analogues **23**, **25**, and **27** is partially quenched. The nature of the quenching mechanism in these complexes is discussed further below. Insertion of the first phenyleneethynylene unit leads to a marked increase of the excited state lifetime, from 150 ns for **9** to 690 ns for **10**. Insertion of the second and third phenyleneethynylene groups in **11**

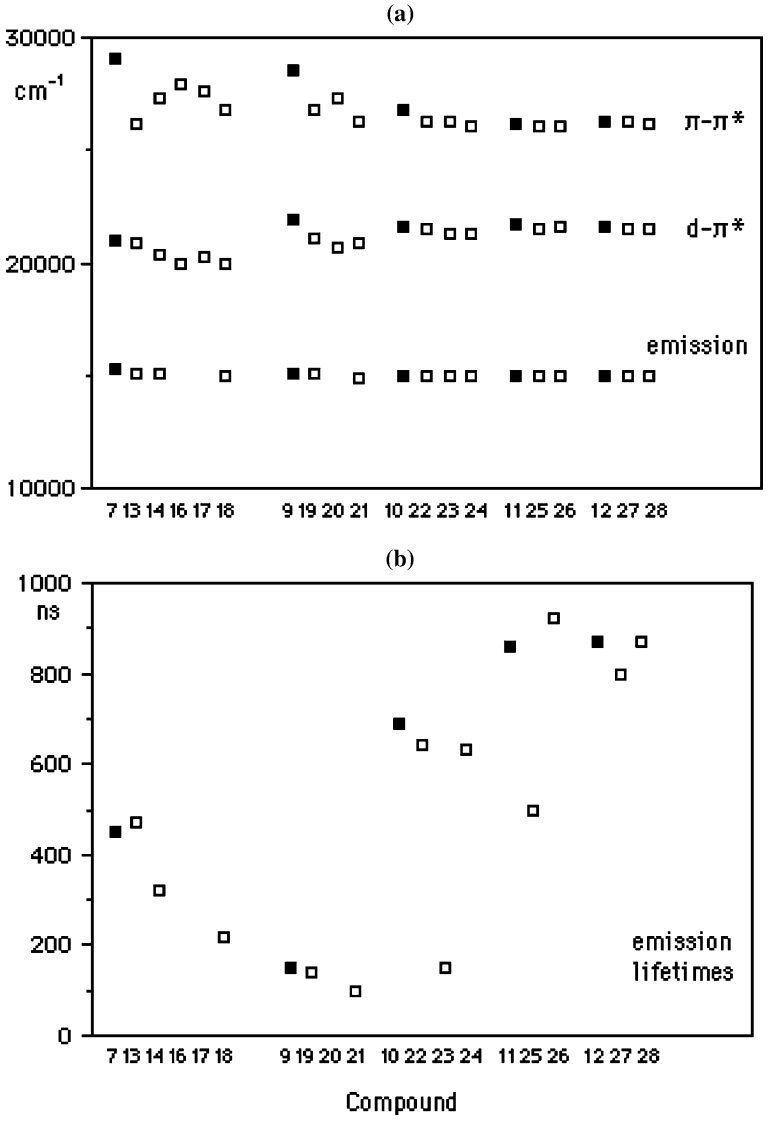

Fig. 5. (a) Plot of the absorption and emission energies (in wavenumbers) of selected compounds. (b) Plot of the emission lifetimes (in nanoseconds) of selected compounds.

Table 5
UV/Vis spectroscopic and electrochemical data of the metal isocyanide complexes **29–33**

Compound	λ/nm (ε/$M^{-1}cm^{-1}$); CH_2Cl_2	E_{red}/V vs. SCE; THF
29	336 (5000, sh), 296 (10300, sh)	
30	344 (4290, sh), 326 (8410, sh), 310 (10500, sh)	−1.866
31	320 (1350), 284 (6440, sh)	−1.150
32	422 (100, sh), 352 (2000), 292 (30600)	−1.143
33	500 (60, sh), 402 (1390, sh), 354 (10700), 262 (72300)	−1.503

sh = shoulder.

and **12** still leads to longer lifetimes of 860 and 870 ns, respectively. The increase in emission lifetime with increasing length of the OPE chain in the series **9–12** is likely the result of an increasing participation of the intraligand character of the extended π-conjugated linkage in the excited state. Within the PdI_2-complex series **20**, **23**, **25** and **27**, there is a special increment to the emission lifetime increase with the extension of the bridge. This may be attributed to a decrease of the efficiency of quenching by the $PdI_2(C\text{-}NAr)_2$ fragment with increasing distance. Nevertheless, even at a separation of 3.1 nm between the tungsten alkylidyne center and the isocyanide-coordinated palladium and platinum centers in **27** and **28**, respectively, the emission lifetime is still about 9% shorter for the PdI_2-containing complex than for the PtI_2-containing complex. Thus, the tungsten alkylidyne fragment is capable of discerning the electronic difference between a palladium and a platinum metal center from a distance of at least 3.1 nm across an isocyanide-terminated oligo-phenyleneethynylene chain.

The tmeda-substitued tungsten alkylidyne complexes are stronger emitters than the dppe-substituted complexes. The luminescence quantum yields of the complexes **7**, **14**, and

18 range from 1.4% to 1.9%, while those of **10**, **22**, and **24** are approximately 0.7%. Naturally, the luminescence quantum yield for the palladium complex **23** is with 0.06% much smaller than that of complex **10**, for example, which is 0.72%. The relative decrease of the luminescence quantum yield between complexes **10** and **23** is approximately the same as the relative decrease of the excited state lifetimes for the same pair of complexes.

3.8. Mechanism of the excited-state quenching by the $PdCl_2(CNArene)_2$ and $PdI_2(CNArene)_2$ fragments

As stated above, the palladium complexes **16**, **17**, and **20** are non-emissive and the extended analogues **23**, **25**, and **27** have reduced emission intensities relative to the parent complexes **10**–**12** as well as the platinum complexes **24**, **26**, and **28**. Evidently, the $PdCl_2(CNAr)_2$ and $PdI_2(CNAr)_2$ units are unique among the tested metal complex fragments in their ability to quench the excited state of the tungsten benzylidyne moiety. As mentioned above, the *trans*-$PdI_2(CNAr)_2$ complex **32** features an absorption tail of very low intensity that extends towards 600 nm. This region overlaps slightly with the emission band of the tungsten benzylidyne complexes. Thus, there exists the possibility of the presence of a low-lying ligand-field triplet state in the palladium moiety of **17** and **20** which deactivates the excited state of the tungsten benzylidyne fragments via energy transfer [28]. However, the *cis*-$PdCl_2(CNAr)_2$ complex **31** does not absorb at wavelengths longer than 450 nm. Consequently, energy transfer is not a viable mechanism of quenching in complex **16**. For **16**, the likely quenching mechanism is therefore electron transfer.

In order to provide supporting evidence for the possible presence of an electron transfer quenching mechanism, the electrochemical properties of the isocyanide metal complexes **29**–**33** were investigated. The results are summarized in Table 5. These compounds exhibit irreversible one-electron reduction waves. In particular, the data show that the palladium bis-isocyanide fragments are significantly more readily reduced, i.e., stronger oxidizing agents, than the rhenium and platinum bis-isocyanide fragments. It is interesting to note that the IR stretching frequencies of the isocyanide groups, which reflect the electron acceptor abilities of the metal centers as Lewis acids, also indicate that the palladium metal centers are the strongest electron acceptors. For the tungsten benzylidyne complexes $W(CC_6H_4I\text{-}4)Cl(CO)_2(tmeda)$ and $W(CC_6H_4I\text{-}4)Cl(CO)_2(dppe)$, which may serve as models for the tungsten alkylidyne fragments in the heteronuclear complexes, irreversible one-electron oxidation waves were observed at +0.91 and +1.01 V versus SCE, respectively. In a larger series of tungsten alkylidyne complexes, the potential of this oxidation was found to be moderately affected by the nature of the donor ligands on tungsten, but only slightly by an extension of the benzylidyne ligand [29]. Consequently, the oxidation waves are assigned to one-electron oxidations of the tungsten centers. The oxidation potential of the excited tungsten alkylidyne fragment, $E(W^+/W^*)$, may be approximated as $E(W^+/W^0) - \Delta E_{0-0}$. With oxidation potentials $E(W^+/W^0)$ of about +1 V versus SCE for the tungsten benzylidyne model complexes and estimated 0–0 excitation energies near 18 200 cm^{-1} (550 nm, 2.26 eV), $E(W^+/W^*)$ may be estimated to be about −1.26 V versus SCE. Thus, $E(Ox/Ox^-) - E(W^+/W^*) = \Delta E > 0$ for the palladium complexes, but $\Delta E < 0$ for the rhenium and platinum complexes [30]. Consequently, electron transfer is thermodynamically favorable in the palladium complexes, but not in the rhenium and platinum systems. Thus, the electrochemical data confirm the conclusion that electron transfer is the most likely mechanism of quenching in **16**. In addition, these data show that electron transfer is also a feasible quenching mechanism in the palladium diiodide complexes **17**, **20**, **23**, **25**, and **27**. Given the fact that the reduction potentials of the palladium complexes **31** and **32** are very similar, it appears likely that electron transfer is also the active quenching mechanism in the palladium diiodide complexes. Preference of electron transfer over energy transfer in systems where both are in principle possible has been observed in other cases [31].

The rate constants of the observed emissions are the inverse of the emission lifetimes (Eq. (1)). It seems reasonable to assume that the excited state decay processes in the palladium complexes **23**, **25**, and **27** and in the corresponding parent complexes **10**–**12** are the same except for the additional independent quenching mechanism in the palladium complexes. This assumption is supported by the observation that the diiodoplatinum unit in complexes **21**, **24**, **26**, and **28**, which is not capable of quenching the emission but otherwise has electronic properties that are very similar to those of the diiodopalladium unit, does not significantly affect the emission properties of the respective parent systems **9**–**12**. Thus, the rate constants of the quenching processes are the differences between the emission rate constants of the palladium complexes and those of the corresponding parent complexes (Eq. 2).

$$k_{em} = 1/\tau, \tag{1}$$

$$k = k_{em}(Pd) - k_{em}(Parent), \tag{2}$$

$$k' = k_{em}(Parent) \times [\phi(Parent) - \phi(Pd)]/[\phi(Pd)], \tag{3}$$

$$k(d) = k_0 e^{-\beta d}. \tag{4}$$

In an alternative procedure the relative loss of quantum yield of emission in the palladium and the corresponding parent compounds is used to estimate the rate constants of the quenching process (Eq. (3)) [32]. The calculated quenching rate constants based on Eqs. (2) and (3) for

Table 6
Calculated rate constants k and k' for the quenching processes using Eqs. (2) and (3), respectively

Compound	k ($\times 10^5$ s^{-1})	k' ($\times 10^5$ s^{-1})
23	69	160
25	8.4	8.9
27	1.0	0.35

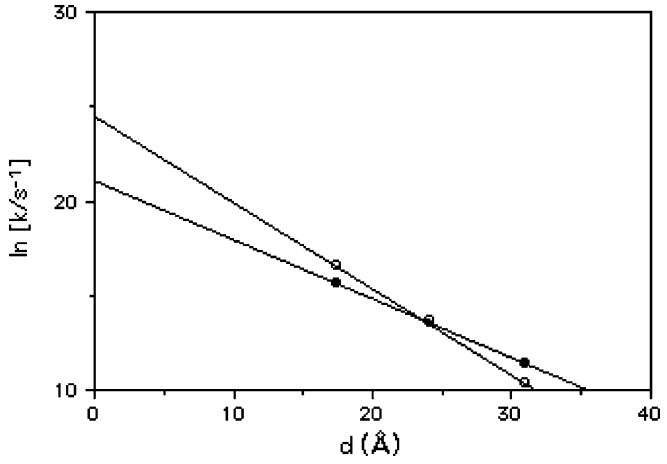

Fig. 6. Plot of $\ln[k/s^{-1}]$ vs. the W–Pd distance for **23**, **25**, and **27**. Full circles: data obtained via Eq. (2). Open circles: data obtained via Eq. (3).

complexes **23**, **25**, and **27** are listed in Table 6. The linear plots of the respective $\ln[k/s^{-1}]$ values versus the W–Pd distances d (Fig. 6) show that the distance dependences of the quenching rate constants may be described by Eq. (4). With a W–Pd distance of 10.5 Å in complex **17** and an increment of 6.8 Å for each phenyleneethynylene unit, the W–Pd distances in **23**, **25**, and **27** are estimated to be 17.3, 24.1, and 30.9 Å, respectively. The resulting attenuation factors β and β' of the distance dependences are 0.31 $Å^{-1}$ and 0.45 $Å^{-1}$, respectively. Considering that the intrinsic experimental errors of the luminescence intensity measurements are about 10% and even larger when the intensity is low, such as in compound **23**, these two values are in reasonable agreement. These values also fall into the range of ~0.2–0.6 $Å^{-1}$ of previously reported experimental and theoretical β values for electron transfer processes across OPE bridges [33]. Thus, an electron transfer mechanism for the quenching process is consistent with the results.

4. Conclusions

The electronic communication between the metal centers in complexes of the general type $L_nW{\equiv}C{-}C_6H_4({-}C{\equiv}C{-}C_6H_4)_p{-}N{\equiv}C{-}M'L'_m$ has been explored. The influence of the isocyanide metal complex fragment on the tungsten alkylidyne complex fragment has been tested by a variety of spectroscopic methods and the dependence of spectroscopic parameters on the number of inserted ethynylenephenylene units has been evaluated.

For probing the long-range electronic communication between the metal centers, the emission property of the tungsten alkylidyne fragment provides the most sensitive parameters, provided the isocyanide metal complex fragment is capable of quenching the emission of the tungsten alkylidyne fragment. This is the case with the palladium(II) fragments $PdCl_2(CNAr)_2$ and $PdI_2(CNAr)_2$. In the complexes containing these fragments, electron transfer is the most likely quenching mechanism. Partial quenching is still readily discerned at a distance of more than 3 nm between the tungsten and palladium metal centers.

The influence of the isocyanide-coordinated metal centers on the alkylidyne $d \rightarrow \pi^*$ and $\pi \rightarrow \pi^*$ transitions diminishes rapidly with increasing separation. By means of these spectroscopic parameters a clear distinction between different isocyanide-coordinated metal centers is still possible after insertion of the first ethynylphenylene spacer, at metal–metal distances of about 1.6 nm. However, residual effects are still discernible at the largest investigated distances of about 3.1 nm. Using the ^{13}C NMR chemical shift of the alkylidyne carbon atom as a reporter, the ability to distinguish between different isocyanide-coordinated metal centers has nearly vanished after insertion of the first phenyleneethynylene group, although the extension of the π system by a second phenyleneethynylene group does induce a characteristic downfield increment.

Those spectroscopic parameters of the tungsten alkylidyne fragment that are not directly associated with the metal–alkylidyne π system, such as the IR stretches of the carbonyl ligands or the ^{31}P NMR chemical shifts of the dppe ligand, are quite insensitive to modifications of the isocyanide-coordinated metal centers, even in the parent isocyanobenzylidyne systems.

Acknowledgements

Support for this work by the Committee on Conference and Research Grants of The University of Hong Kong and by the Hong Kong Research Grants Council is gratefully acknowledged.

Appendix A. Supplementary data

Crystallographic data for the structural analysis of compound **17** have been deposited with the Cambridge Crystallographic Data Centre, CCDC No. 293397. Supplementary data associated with this article can be found, in the online version, at doi:10.1016/j.jorganchem.2006.02.029.

References

[1] (a) D.M. Adams, L. Brus, C.E.D. Chidsey, S. Creager, C. Creutz, C.R. Kagan, P.V. Kamat, M. Lieberman, S. Lindsay, R.A. Marcus, R.M. Metzger, M.E. Michel-Beyerle, J.R. Miller, M.D. Newton, D.R. Rolison, O. Sankey, K.S. Schanze, J. Yardley, X. Zhu, J. Phys. Chem. B 102 (2003) 6668;
(b) D. Holten, D.F. Bocian, J.S. Lindsey, Acc. Chem. Res. 35 (2002) 57;
(c) J. Tour, Molecular Electronics, World Scientific, Singapore, 2003.
[2] (a) C. Creutz, Prog. Inorg. Chem. 30 (1983) 1;
(b) J.R. Miller, J.V. Beitz, R.K. Huddleston, J. Am. Chem. Soc. 106 (1984) 5057;
(c) M.D. Newton, Chem. Rev. 91 (1991) 767;
(d) J.R. Winkler, H.B. Gray, Chem. Rev. 92 (1992) 369;
(e) M.R. Wasielewski, Chem. Rev. 92 (1992) 435;
(f) J.-P. Sauvage, J.-P. Collin, J.-C. Chambron, S. Guillerez, C. Coudret, Chem. Rev. 94 (1994) 993;
(g) D. Astruc, Acc. Chem. Res. 30 (1997) 383;
(h) R. Ziessel, M. Hissler, A. El-ghayoury, A. Harriman, Coord. Chem. Rev. 178–180 (1998) 1251;

(i) J.D. Badjic, A. Nelson, S.J. Cantrill, W.B. Turnbull, J.F. Stoddart, Acc. Chem. Res. 38 (2005) 723.
[3] (a) C. Liang, M.D. Newton, J. Phys. Chem. 97 (1993) 3199;
(b) B.P. Paulson, L.A. Curtiss, B. Bal, G.L. Closs, J.R. Miller, J. Am. Chem. Soc. 118 (1996) 378.
[4] (a) M.V. Barybin, M.H. Chisholm, N.S. Dalal, T.H. Holovics, N.J. Patmore, R.E. Robinson, D.J. Zipse, J. Am. Chem. Soc. 127 (2005) 15182;
(b) G.-L. Xu, R.J. Crutchley, M.C. DeRosa, Q.-J. Pan, H.-X. Zhang, X. Wang, T. Ren, J. Am. Chem. Soc. 127 (2005) 13354;
(c) T. Sheng, H. Vahrenkamp, Eur. J. Inorg. Chem. (2004) 1198;
(d) E.C. Constable, E. Figgemeier, C.E. Housecroft, J. Olsson, Y.C. Zimmermann, Dalton Trans. (2004) 1918.
[5] (a) W. Beck, B. Niemer, M. Wieser, Angew. Chem. 105 (1993) 969; Angew. Chem., Int. Ed. Engl. 33 (1993) 547;
(b) S.H. Liu, Y. Chen, K.L. Wan, T.B. Wen, Z. Zhou, M.F. Lo, I.D. Williams, G. Jia, Organometallics 21 (2002) 4984;
(c) M.-C. Chung, X. Gu, B.A. Etzenhouser, A.M. Spuches, P.T. Rye, S.K. Seetharaman, D.J. Rose, J. Zubieta, M.B. Sponsler, Organometallics 22 (2003) 3485.
[6] (a) A. Mayr, M.P.Y. Yu, V.W.-W. Yam, J. Am. Chem. Soc. 121 (1999) 1760;
(b) Z. Xu, A. Mayr, I.S. Butler, J. Organomet. Chem. 648 (2002) 93;
(c) Z. Xu, I.S. Butler, A. Mayr, Spectrochim. Acta A 61 (2005) 995.
[7] (a) E.O. Fischer, Angew. Chem. 86 (1974) 651;
E.O. Fischer, Adv. Organomet. Chem. 14 (1976) 1;
(b) H. Fischer, P. Hofmann, F.R. Kreissl, R.R. Schrock, U. Schubert, K. Weiss, Carbyne Complexes, VCH, Weinheim, 1988;
(c) W.A. Nugent, J.M. Mayer, Metal–Ligand Multiple Bonds, Wiley, New York, 1988;
(d) H.P. Kim, R.J. Angelici, Adv. Organomet. Chem. 27 (1987) 51;
(e) A. Mayr, H. Hoffmeister, Adv. Organomet. Chem. 32 (1991) 227;
(f) A. Mayr, S. Ahn, Adv. Trans. Met. Coord. Chem. 1 (1996) 1;
(g) R.R. Schrock, J. Chem. Soc., Dalton Trans. (2001) 2541;
(h) J.W. Herndon, Coord. Chem. Rev. 249 (2005) 999.
[8] (a) E.O. Fischer, W. Roll, N.H.T. Huy, K. Ackermann, Chem. Ber. 115 (1982) 2951;
(b) N.A. Ustynyuk, V.N. Vinograda, V.G. Andrianov, Y.T. Struchkov, J. Organomet. Chem. 268 (1984) 73;
(c) S.A. Krouse, R.R. Schrock, J. Organomet. Chem. 355 (1988) 257;
(d) M.H. Chisholm, J.C. Huffman, J.A. Klang, Polyhedron 9 (1990) 1271;
(e) T.M. Gilbert, R.D. Rogers, J. Organomet. Chem. 421 (1991) C1;
(f) B.E. Woodworth, P.S. White, J.L. Templeton, J. Am. Chem. Soc. 119 (1997) 828;
(g) S.B. Falloon, W. Weng, A.M. Arif, J.A. Gladysz, Organometallics 16 (1997) 2008;
(h) D.A. Valyaev, M.G. Peterleitner, L.I. Leont'eva, L.N. Novikova, O.V. Semeikin, V.N. Khrustalev, M.Y. Antipin, N.A. Ustynyuk, B.W. Skelton, A.H. White, Organometallics 22 (2003) 5491;
(i) K. Venkatesan, O. Blacque, T. Fox, M. Alfonso, H.W. Schmalle, S. Kheradmandan, H. Berke, Organometallics 24 (2005) 920.
[9] (a) R.E. Da Re, M.D. Hopkins, Coord. Chem. Rev. 249 (2005) 1396;
(b) A. Vogler, J. Kisslinger, W.R. Roper, Z. Naturforsch. B 38B (1983) 1506;
(c) A.B. Bocarsly, R.E. Cameron, H.-D. Rubin, G.A. McDermott, C.R. Wolff, A. Mayr, Inorg. Chem. 24 (1985) 3976;
(d) A.B. Bocarsly, R.E. Cameron, A. Mayr, G.A. McDermott, in: H. Yersin, A. Vogler (Eds.), Photochemistry and Photophysics of Coordination Compounds, Springer, Berlin, 1987;
(e) J.D. Carter, K.B. Kingsbury, L. McElwee-White, J. Am. Chem. Soc. 113 (1991) 2947;
(f) T.K. Schoch, A.D. Main, R.D. Burton, L.A. Lucia, E.A. Robinson, K.S. Schanze, L. McElwee-White, Inorg. Chem. 35 (1996) 7769;
(g) C.C.S. Cavalheiro, K.E. Torraca, K.S. Schanze, L. McElwee-White, Inorg. Chem. 38 (1999) 3254;
(h) J. Manna, S.J. Geib, M.D. Hopkins, J. Am. Chem. Soc. 114 (1992) 9199;
(i) T.P. Pollagi, S.J. Geib, M.D. Hopkins, J. Am. Chem. Soc. 116 (1994) 6051;
(j) H.A. Brison, T.P. Pollagi, T.C. Stoner, S.J. Geib, M.D. Hopkins, Chem. Commun. (1997) 1263;
(k) K.D. John, M.D. Hopkins, Chem. Commun. (1999) 589;
(l) S. Trammell, B.P. Sullivan, L.M. Hodges, W.D. Harman, S.R. Smith, H.H. Thorp, Inorg. Chem. 34 (1995) 2791;
(m) W.-M. Xue, Y. Wang, T.C.W. Mak, C.-M. Che, J. Chem. Soc., Dalton Trans. (1996) 2827;
(n) W.-M. Xue, M.C.W. Chan, T.C.W. Mak, C.-M. Che, Inorg. Chem. 36 (1997) 6437;
(o) W.-M. Xue, Y. Wang, M.C.-W. Chan, Z.-M. Su, K.-K. Cheung, C.-M. Che, Organometallics 17 (1998) 1946;
(p) F.-W. Lee, M.C.-W. Chan, Z.-M. Su, K.-K. Cheung, C.-M. Che, J. Organomet. Chem. 552 (1998) 255;
(q) F.W. Lee, M.C.-W. Chan, K.-K. Cheung, C.-M. Che, J. Organomet. Chem. 563 (1998) 191;
(r) S.-W. Lai, M.C.-W. Chan, Y. Wang, H.-W. Lam, S.-M. Peng, C.-M. Che, J. Organomet. Chem. 617–618 (2001) 133;
(s) C.K. Simpson, R.E. Da Re, T.P. Pollagi, I.M. Steele, R.F. Dallinger, M.D. Hopkins, Inorg. Chim. Acta 345 (2003) 309.
[10] (a) P.M. Treichel, Adv. Organomet. Chem. 11 (1973) 21;
(b) F.A. Cotton, F. Zingales, J. Am. Chem. Soc. 83 (1961) 83, 351;
(c) D. Moigno, B. Callejas-Gasper, J. Gil-Rubio, H. Werner, W. Kiefer, J. Organomet. Chem. 661 (2002) 181.
[11] (a) E. Singleton, H.E. Oosthuizen, Adv. Organomet. Chem. 22 (1983) 209;
(b) W.P. Fehlhammer, M. Fritz, Chem. Rev. 93 (1993) 193.
[12] (a) L.-F. Mao, A. Mayr, Inorg. Chem. 35 (1996) 3183;
(b) J. Guo, A. Mayr, Inorg. Chim. Acta 261 (1997) 141;
(c) A. Mayr, L.-F. Mao, Inorg. Chem. 37 (1998) 5776;
(d) S. Wang, A. Mayr, K.-K. Cheung, J. Mater. Chem. 8 (1998) 1561;
(e) K.Y. Lau, A. Mayr, K.-K. Cheung, Inorg. Chim. Acta 285 (1999) 223;
(f) Z.-L. Lu, A. Mayr, K.-K. Cheung, Inorg. Chim. Acta 284 (1999) 205;
(g) L. Yang, K.-K. Cheung, A. Mayr, J. Organomet. Chem. 585 (1999) 26;
(h) A. Mayr, J. Guo, Inorg. Chem. 38 (1999) 921;
(i) Y.-B. Dong, L. Yang, K.-K. Cheung, A. Mayr, J. Organomet. Chem. 598 (2000) 55;
(j) M.-X. Li, K.-K. Cheung, A. Mayr, J. Solid State Chem. 152 (2000) 247;
(k) A. Mayr, S. Wang, K.-K. Cheung, M. Hong, J. Organomet. Chem. 684 (2003) 287.
[13] (a) D.K. James, J.M. Tour, Top. Curr. Chem. 257 (2005) 33;
(b) C.D. Zangmeister, S.W. Robey, R.D. van Zee, Y. Yao, J.M. Tour, J. Phys. Chem. B 108 (2004) 16187;
(c) A.M. Funston, E.E. Silverman, J.R. Miller, K.S. Schanze, J. Phys. Chem. B 108 (2004) 1544.
[14] (a) P.F.H. Schwab, M.D. Levin, J. Michl, Chem. Rev. 99 (1999) 1863;
(b) U. Ziener, A. Godt, J. Org. Chem. 62 (1997) 6137.
[15] (a) S.C.-F. Lam, V.W.-W. Yam, K.M.-C. Wong, E.C.-C. Cheng, N. Zhu, Organometallics 24 (2005) 4298;
(b) V.W.-W. Yam, Compt. Rend. Chim. 8 (2005) 1194;
(c) V.W.-W. Yam, J. Organomet. Chem. 689 (2004) 1393;
(d) K.-L. Cheung, S.-K. Yip, V.W.-W. Yam, J. Organomet. Chem. 689 (2004) 4451;
(e) Q. Zheng, J.A. Gladysz, J. Am. Chem. Soc. 127 (2005) 10508;
(f) K.M.-C. Wong, S.C.-F. Lam, C.-C. Ko, N. Zhu, V.W.-W. Yam, S. Roué, C. Lapinte, S. Fathallah, K. Costuas, S. Kahlal, J.-F. Halet, Inorg. Chem. 42 (2003) 7086;
(g) F. De Montigny, G. Argouarch, K. Costuas, J.-F. Halet, T. Roisnel, L. Toupet, C. Lapinte, Organometallics 24 (2005) 4558.
[16] (a) O. Lavastre, L. Ollivier, P. Dixneuf, S. Sibandhit, Tetrahedron 52 (1996) 5495;

(b) I. Ugi, U. Fetzer, U. Eholzer, H. Knupfer, K. Offerman, Angew. Chem. 77 (1965) 492–504.
[17] (a) Z.-L. Lu, A. Mayr, K.-K. Cheung, Inorg. Chim. Acta 284 (1999) 205;
(b) M.P.Y. Yu, K.-K. Cheung, A. Mayr, J. Chem. Soc., Dalton Trans. (1998) 2373;
(c) M.P.Y. Yu, A. Mayr, K.-K. Cheung, J. Chem. Soc., Dalton Trans. (1998) 475;
(d) A. Mayr, M.P.Y. Yu, J. Organomet. Chem. 577 (1999) 223.
[18] (a) C.A. Parker, W.T. Rees, Analyst (London) 85 (1960) 587;
(b) C.A. Parker, Photoluminescence of Solutions, Elsevier, New York, 1968.
[19] A. Harriman, J. Chem. Soc., Chem. Commun. 777 (1977).
[20] N.G. Connelly, W.E. Geiger, Chem. Rev. 96 (1996) 877.
[21] SIR-92: A. Altomare, M. Cascarano, C. Giacovazzo, A. Guagliardi, M.C. Burla, G. Polidori, M. Camalli, J. Appl. Crystallogr. 27 (1994) 435.
[22] TEXSAN: Crystal Structure Analysis Package, Molecular Structure Corporation, 1985 and 1992.
[23] E.O. Fischer, U. Schubert, J. Organomet. Chem. 100 (1975) 59.
[24] (a) N.M. Kostic, R.F. Fenske, Organometallics 1 (1982) 489;
(b) J. Ushio, H. Nakatsuji, T. Yonezawa, J. Am. Chem. Soc. 106 (1984) 5892;
(c) J.M. Poblet, A. Strich, R. Wiest, M. Benard, Chem. Phys. Lett. 126 (1986) 169;
(d) S.F. Vyboishchikov, G. Frenking, Chem. Eur. J. 4 (1998) 1439.
[25] F.W. Wehrli, T. Wirthlin, Interpretation of Carbon-13 NMR Spectra, Heyden, London, 1980.
[26] J.B. Sheridan, D.B. Pourreau, G.L. Geoffroy, A.L. Rheingold, Organometallics 7 (1988) 289.
[27] A. Mayr, C.M. Bastos, R.T. Chang, J.X. Haberman, K.S. Robinson, D.A. Belle-Oudry, Angew. Chem., Int. Ed. Engl. 31 (1992) 747.
[28] A.B.P. Lever, Inorganic Electronic Spectroscopy, second ed., Elsevier, Amsterdam, 1984.
[29] Y.P. Yin, Ph.D. Thesis, The University of Hong Kong, 1998.
[30] (a) A.J. Lees, Chem. Rev. 87 (1987) 711;
(b) M.A. Fox, M. Chanon (Eds.), Photoinduced Electron Transfer, Part A: Conceptual Basis, Elsevier, Amsterdam, 1988.
[31] K.S. Schanze, G.A. Neyhart, T.J. Meyer, J. Phys. Chem. 90 (1986) 2182.
[32] H. Oevering, M.N. Paddon-Row, M. Heppener, A.M. Oliver, E. Cotsaris, J.W. Verhoeven, N.S. Hush, J. Am. Chem. Soc. 109 (1987) 3258.
[33] (a) S.B. Sachs, S.P. Dudek, R.P. Hsung, L.R. Sita, J.F. Smalley, M.D. Newton, S.W. Feldberg, C.E.D. Chidsey, J. Am. Chem. Soc. 119 (1997) 10563;
(b) M. Magoga, C. Joachim, Phys. Rev. B 56 (1997) 4722;
(c) S. Creager, C.J. Yu, C. Bamdad, S. O'Connor, T. MacLean, E. Lam, Y. Chong, G.T. Olsen, J. Luo, M. Gozin, J.F. Kayyem, J. Am. Chem. Soc. 121 (1999) 1059;
(d) J.F. Smalley, S.B. Sachs, C.E.D. Chidsey, S.P. Dudek, H.D. Sikes, S.E. Creager, C.J. Yu, S.W. Feldberg, M.D. Newton, J. Am. Chem. Soc. 126 (2004) 14620;
(e) K. Pettersson, J. Wiberg, T. Ljungdahl, J. Martensson, B. Albinnson, J. Phys. Chem. A 110 (2005) 319.